Gondwana Research 109 (2022) 150–165

Contents lists available at ScienceDirect

Gondwana Research

journal homepage: www.elsevier.com/locate/gr

GR Focus Review

Atmospheric dust dynamics over Central Asia: A perspective view from loess deposits

Yue Li [a,b], Yougui Song [a,c,*], Dimitris G. Kaskaoutis [d,e], Xiaoxiao Zhang [f,g], Xiuling Chen [h], Nosir Shukurov [i], Rustam Orozbaev [j]

[a] State Key Laboratory of Loess and Quaternary Geology, Institute of Earth Environment, Chinese Academy of Sciences, Xi'an 710061, China
[b] Key Laboratory of Desert and Desertification, Northwest Institute of Eco-Environment and Resources, Chinese Academy of Sciences, Lanzhou 730000, China
[c] CAS Center for Excellence in Quaternary Science and Global Change, Xi'an 710061, China
[d] Institute for Environmental Research and Sustainable Development, National Observatory of Athens, Athens 11810, Greece
[e] Environmental Chemical Processes Laboratory, Department of Chemistry, University of Crete, Crete 71003, Greece
[f] State Key Laboratory of Desert and Oasis Ecology, Xinjiang Institute of Ecology and Geography, Chinese Academy of Sciences, Urumqi 830011, China
[g] State Key Laboratory of Atmospheric Boundary Layer Physics and Atmospheric Chemistry, Institute of Atmospheric Physics, Chinese Academy of Sciences, Beijing 100029, China
[h] State Key Laboratory for Subtropical Mountain Ecology of the Ministry of Science and Technology and Fujian Province, Fujian Normal University, Fuzhou 350007, China
[i] Institute of Geology and Geophysics, University of Geological Sciences, State Committee of the Republic of Uzbekistan for Geology and Mineral Resources, Tashkent 100041, Uzbekistan
[j] Institute of Geology, National Academy of Sciences of Kyrgyz Republic, Bishkek 720040, Kyrgyzstan

ARTICLE INFO

Article history:
Received 1 December 2021
Revised 8 April 2022
Accepted 28 April 2022
Available online 4 May 2022
Handling Editor: Y.J. Liu

Keywords:
Central Asian loess
Westerly jet
Siberian high
NAO/AO
CasHKI

ABSTRACT

Different origins of loess deposits in northern and southern Central Asia are not only associated with Central Asian topography, but also with aeolian dust dynamics. However, the latter has received far less attention so far. This review focuses on atmospheric dust dynamics for loess deposition in Central Asia, aiming to heal this knowledge gap. Comparisons of loess grain size data from the Chinese Loess Plateau, and the northern and southern Central Asia suggested that the Siberian High-pressure system largely controlled dust mobilization and loess accumulation in northern Central Asia, instead of southern Central Asia. The North Atlantic Oscillation (NAO) mode also provided an additional promising solution to trigger of loess accumulation in the North Tianshan Mountains. In southern Central Asia, intensity of dust activity was majorly determined by the Caspian Sea-Hindu Kush Index (CasHKI), with stronger dust dynamics under higher CasHKI modes. However, the causes of variations in the CasHKI intensity represent a future challenge. The CasHKI values also influenced the wind dynamics controlling dust mobilization in the Fergana Valley. Therefore, the Central Asia can be divided into two parts regarding the aeolian dust dynamics, with a boundary located in the North Tianshan Mountains and the south of Aral Sea. The Siberian High and NAO phase appeared to affect the dust activity and loess accumulation in the northern part; while dust entrainment and deposition were mostly determined by the CasHKI mode in the southern part. However, precisely determining the boundary highlights the necessity of investigations on loess deposits in the Tashkent region. In addition, we further recommend that the dynamic linkages between the mid-latitude Westerlies and aeolian loess deposition constitute a future critical research topic in Central Asia.

Contents

Abbreviations: NAO, North Atlantic Oscillation; AO, Arctic oscillation; CasHKI, Caspian Sea-HinduKush Index.

* Corresponding author at: State Key Laboratory of Loess and Quaternary Geology, Institute of Earth Environment, Chinese Academy of Sciences, No. 97 Yanxiang Road, Yanta, Xi'an 710061, China.
E-mail address: syg@ieecas.cn (Y. Song).

https://doi.org/10.1016/j.gr.2022.04.019
1751-7311/

1. Introduction

The belt with arid climate extending from the western Sahara to the northwestern China and southern Mongolia is a major dust source in the Northern Hemisphere (Engelbrecht and Derbyshire, 2010; Prospero et al., 2002; Shi et al., 2021). A better understanding of variability of dust emission and a more detailed analysis of dust dynamics in this belt can elevate our knowledge of patterns and drivers of global dust cycle (Engelstaedter et al., 2006; Marx et al., 2018). Central Asia (CA), zonally extending from the Caspian Sea to East Tianshan Mountains, is located in the eastern end of the dust belt. The frequently-occurred and rather intensive sand and dust storms in CA, which are estimated to contribute to 17–20% of global dust emissions (Ge et al., 2016; Indoitu et al., 2012; Issanova et al., 2015; Li and Sokolik, 2018; Pi et al., 2017; Shen et al., 2016; Shi et al., 2020; Xi and Sokolik, 2015a,b; Zhang et al., 2020) have attracted broad scientific interests due to their influences on socioeconomics, human health, and ecosystems (Goudie, 2014; Groll et al., 2013; Indoitu et al., 2015; Issanova and Abuduwaili, 2017; Opp et al., 2017; Shen et al., 2016; Zhang et al., 2020), particularly motivating numerous studies on dust activity and associated land and atmospheric characteristics and dynamics (Gholami et al., 2021; Groll et al., 2013; Li et al., 2019a; Shi et al., 2020). However, at present, dust variability over CA are related to interactions between natural processes and human activities (Gintzburger et al., 2005; Issanova and Abuduwaili, 2017; Lioubimtseva et al., 2005; Liu et al., 2021; Orlovsky and Orlovsky, 2002; Shen et al., 2016; Shi et al., 2020; Xi and Sokolik, 2015a,b). As a result, the respective signals of natural process and human activity and their driving mechanisms are difficult to examine.

To understand the natural processes driving the dust cycle in CA and their roles in the Earth's climate system, paleo-dust deposits or eolian loess sequences deserve special attentions (Fan et al., 2021; Fitzsimmons et al., 2018; Jia et al., 2022; Li et al., 2020a; Li et al., 2019b; Li et al., 2021; Wang et al., 2018b; Yang et al., 2021; Song et al., 2022). Loess constitutes an important geomorphic unit in CA, along the Tian Shan, Alai, Altai and Pamir mountainous ranges (Dodonov, 1991; Li et al., 2015; Song et al., 2021; Song et al., 2014). Recently, according to the disparities of loess composition, climate differences and topographic effects, Song et al. (2021) divided the loess distribution in Central Asia into three subregions (Suppl. Fig. S1): Western CA (Subregion I), Northern CA (Subregion II), and Eastern CA (Subregion III). However, there are so far no well-debated and convincingly-presented propositions to link the three sub-region dividing scheme with atmospheric dynamic processes.

Previous paleoclimatic studies linked dust depositions over the CA region directly to the westerlies (Ding et al., 2002; Li et al., 2016a; Vandenberghe et al., 2006). However, the mountainous ranges in CA lead to variable climate and atmospheric circulation patterns from site to site (Guan et al., 2019; Hamzeh et al., 2016; Issanova and Abuduwaili, 2017; Li et al., 2020c; Rugenstein and Chamberlain, 2018; Sha et al., 2018). Therefore, some debates are now being raised about whether it is possible to simply link the intensity of dust activity to the westerlies in CA. In North Tianshan Mountains, Machalett et al. (2008) argued that the Asiatic polar front influenced past dust storm frequency in northern CA (NCA), while Fitzsimmons et al. (2018) posited that meridional compression of the North Atlantic-influenced Westerlies driven by extended glaciers in the Tianshan Mountains was responsible for accelerated dust accumulation, facilitating increases in loess flux. In the last few years, our group has also been devoting ourselves to resolve aeolian dynamics of loess deposition in the region west of the Tianshan Mountains and Pamirs (Li et al., 2018a, 2019a,b, 2021, Song et al., 2021, 2022). To date, the predominant aeolian dust dynamics in NCA and southern CA (SCA) have been clarified, which are useful for paleoclimatic reconstructions based on proxy indicators of CA loess. We hope that this review/study can become an important basis for the ongoing efforts to better recover and decipher evolutionary history of Quaternary climate in CA.

The paper is organized as follows. Section 2 simply describes regional setting of the study area. Our primary inspiration and motivation for study of atmospheric dust dynamics over CA are introduced in Section 3. The different dust dynamics in the NCA and the SCA are clarified in Section 4, with adding some explanations to aeolian dust dynamics in the NCA. A boundary was distinguished in CA regarding the different atmospheric dust dynamics in Section 5. The conclusions are summarized in Section 6.

2. Regional setting

The area of interest is mainly located in the west of the Tianshan and Pamir mountainous ranges, exclusive of the Tarim Basin; the geographical setting and climate of the region were described in more detail elsewhere (Li et al., 2020c; Song et al., 2021). Uplift of water vapor carried by the mid-latitude westerlies (Guan et al., 2019; Wang et al., 2016), forced by block of the Tianshan Mountains and Pamirs, produces orographic rainfall mostly in windward (western) slopes of the mountains (Fig. 1a). The mean annual precipitation in the mountainous areas is thereby higher and increases with rising elevation on windward (west-facing) slopes (Fig. 1a; Song et al., 2021). As for seasonality of precipitation, more precipitation occurs during the spring/summer in the northern part of CA, with cold and dry winters, while the southern part is characterized by wet winter/spring and hot and dry summer (Lydolph, 1977; Rachkovskaya, 2003) (Fig. 1b). The prevailing westerlies flowing along a SW-NE striking path dominate CA in all seasons except for summer (Dong et al., 2018; Guan et al., 2019; Li et al., 2020b) (Fig. 1c). The westerly circulations entering CA are divided into two branches in summer (Guan et al., 2019). One branch flows into

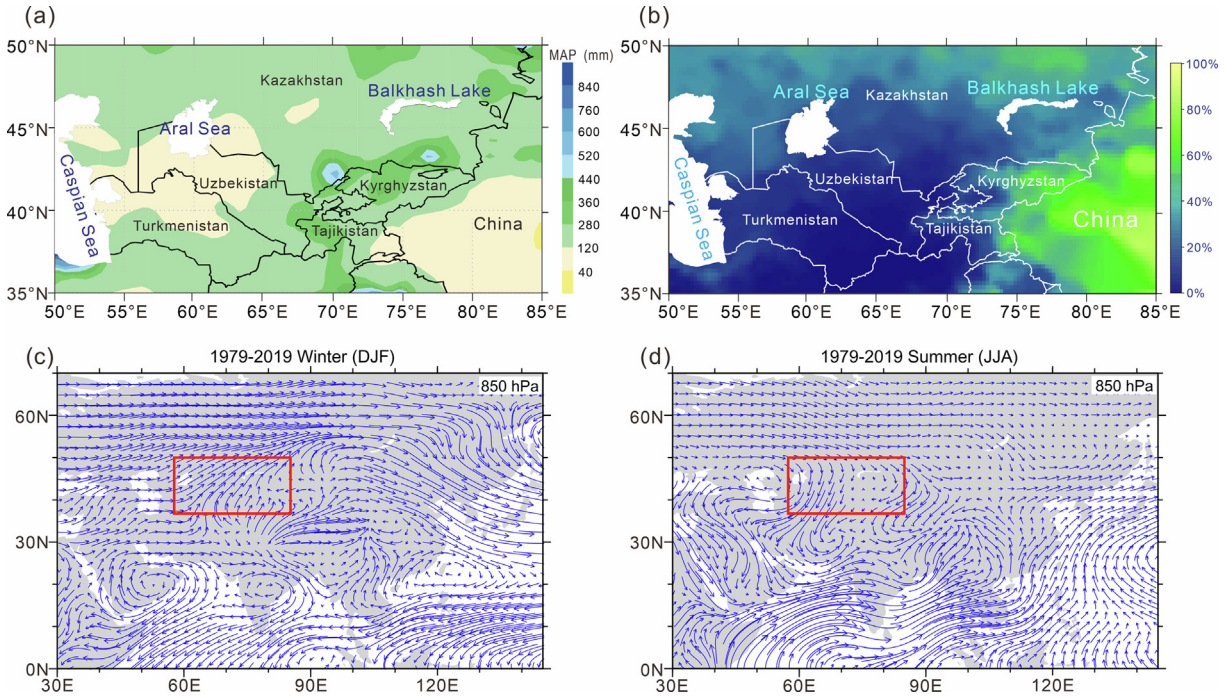

Fig. 1. The spatial distributions of mean annual precipitation (MAP) in Central Asia (CA) (a, URL: https://gmao.gsfc.nasa.gov/reanalysis/MERRA-2/) (After Li et al., 2020c). Proportion of summer (JJA) precipitation to annual precipitation in CA for 1951–2000 (data source: Global Precipitation Climatology Centre Climatology Version 2018 at 0.25° resolution; Meyer-Christoffer et al., 2018) (Modified after Li et al., 2020b). Mean winter (c) and summer (d) streamline (ms^{-1}) at 850 hPa (~1500 m asl) in Asia for the years 1979–2019 (data from the European Centre for Medium-Range Weather Forecasts Re-Analysis-Interim data sets; Dee et al. (2011). Red boxes in the panels refer to the Central Asian region described here.

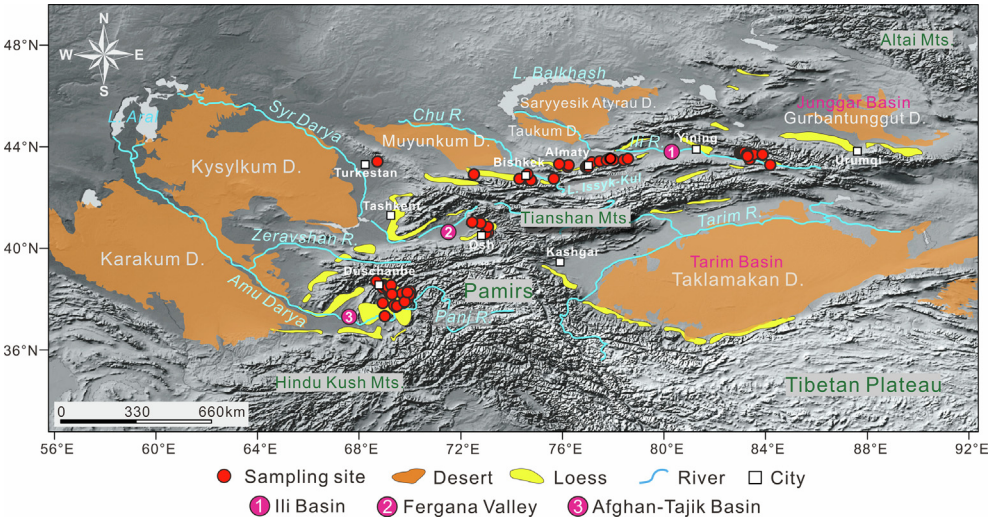

Fig. 2. Geography and sampling locations in Central Asia (After Li and Song, 2021).

eastern CA (Xinjiang region of Northwest China); the other branch outflows from the southwest boundary of CA under the influence of the Iranian trough (high pressure system) and the Caspian Sea High (Fig. 1d), forming the strong seasonal Levar wind from CA to the north Arabian Sea (Hamidianpour et al., 2021; Kaskaoutis et al., 2017).

3. Provenance of loess deposits: A primary motive for investigation of dust dynamics in CA

Many loess samples were taken from the Ili Basin (Northwest China), the northern slopes of the North Tianshan Mountains, the Fergana Valley, and Afghan-Tajik Basin during various field campaigns in 2011, 2013, 2014, 2015, 2017 and 2019 (Li et al., 2020a–c; Song et al., 2021) (Fig. 2). A total of 63 loess samples was used to examine consistency of their geochemical compositions. They included 13 samples from eastern Ili Basin (China), 21 samples from the northern slope of the North Tianshan Mountains (Kazakhstan/Kyrgyzstan), 5 samples from the Fergana Valley (Uzbekistan/Kyrgyzstan) and 24 samples from Afghan-Tajik Basin (Tajikistan) (Fig. 2). The results of trace elements have been reported in Li et al. (2018b), Li et al. (2019a) and Li et al. (2020c). Here, 34 trace elements and 33 (rare earth element) REE parameters and elemental ratios of these loess samples (Table S1) were

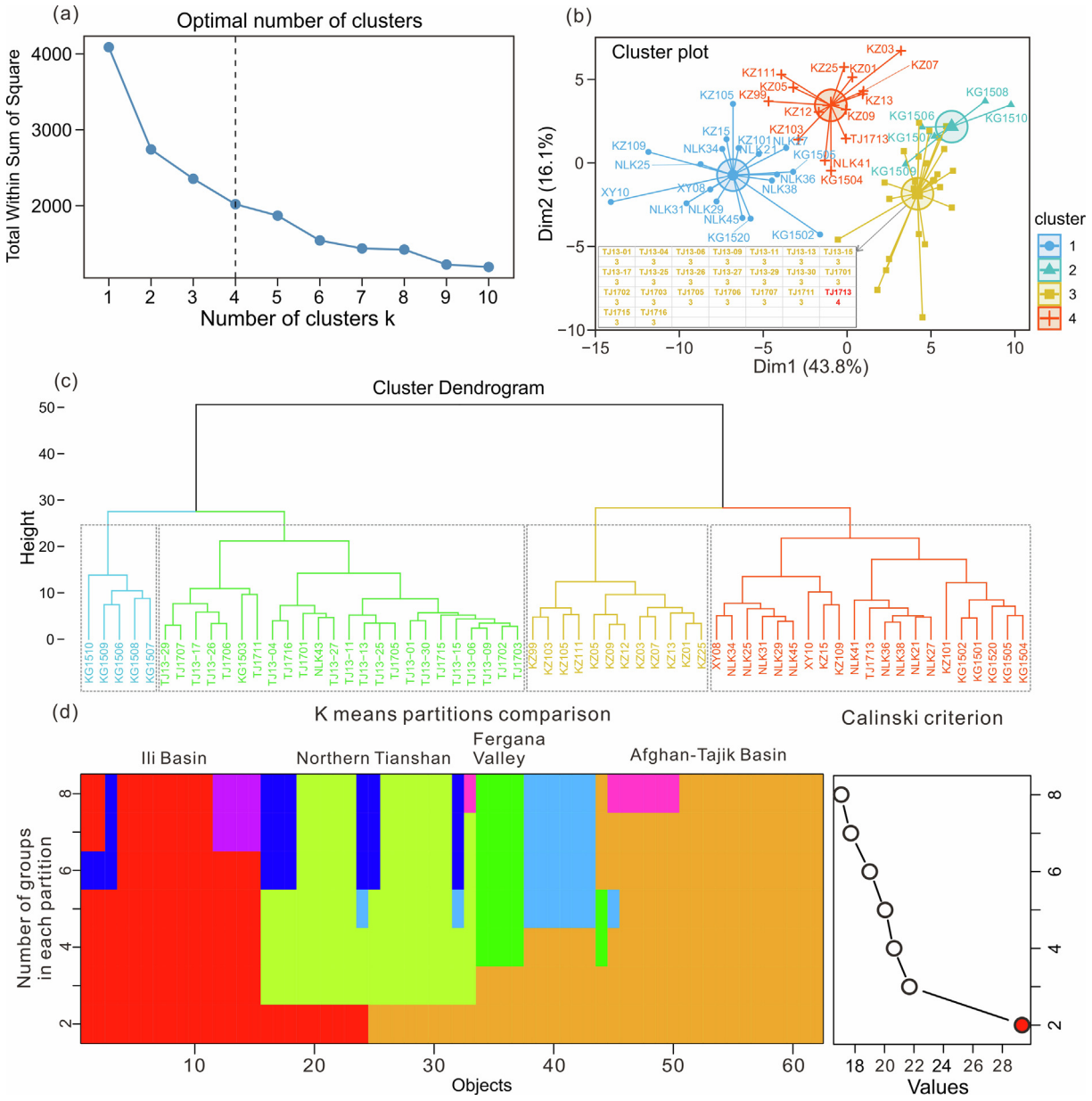

Fig. 3. (a) Determination of optimal number of clusters based on k-means clustering algorithm. (b) Bidimensional cluster plot showing differentiation of four clusters. (c) Cluster dendrogram for hierarchical clustering. (d) K-means partitions comparison and determination of optimal number of clusters based on Calinski-Harabasz criterion.

reconsidered to investigate similarities and differences of their provenances. We calculated the 33 REE parameters and trace element ratios according to previously published studies (see Suppl. Text S1). In total, 67 elements or indexes were available for use in subsequent statistical analyses.

Clustering analysis, an unsupervised learning algorithm, was employed for identifying the clusters with similar trace element compositions. Firstly, the number of clusters k was determined to be 4 (Fig. 3a) due to collection of the loess samples from four sampling regions, as described above. Fig. 3b shows the clear discrimination between the four clusters. More notably, cluster 1 includes all samples from the Ili Basin and some samples from the North Tianshan Mountains, cluster 2 includes the samples from the Fergana Valley, cluster 3 includes almost all of samples from the Afghan-Tajik Basin except for TJ1713, and the cluster 4 includes most of samples from the North Tianshan Mountains (Fig. 3b). Such results were also displayed in cluster dendrogram produced in hierarchical clustering, and overall, the 4 clusters correspond to the 4 sampling regions (Figs. 1 and 3c). Therefore, the results revealed that loess deposits from different regions in CA were characterized by local source-to-sink system (Li and Song, 2021; Li et al., 2018b,2019b,2016b,2020c) and their sources were different between each other. The difference in loessic provenance may be attributed to the complex topography in CA, which results in varying wind trajectories and associated transport of aeolian sediments on a local scale (Li et al., 2018b,2020c). In effect, the geomorphology and topographic patterns of CA does not allow wide-scale loess plateaus to develop (Dodonov, 1991).

We further used the Calinski-Harabasz criterion to determine optimal number of clusters and the results show two identified clusters (Fig. 3d). It was found that samples from the Ili Basin and some samples from the North Tianshan Mountains were divided into one cluster, and all samples from the Fergana Valley and the Afghan-Tajik Basin were categorized into another cluster

(Fig. 3d). Loess sediments in the north part of the Tianshan Mountains thereby have little similarity to the south part. On the one hand, this scenario was thought to be related to influence of CA topography, as stated above. On the other hand, combined with the fact that dust emissions or dust storms have peaks in spring in the eastern and northern parts of CA, and in summer in the western part (Nobakht et al., 2019,2021), the different sources of loess deposits from north and south of the Tianshan Mountains were also likely attributed to distinct atmospheric dust dynamics associated with the climatic circulation systems in different seasons (Fitzsimmons et al., 2020; Li et al., 2021; Lu et al., 2020). Consequently, focusing on the latter, the aeolian dynamics of loess deposition across CA were considered in detail below.

4. Different dust dynamics in the NCA and the SCA

4.1. Atmospheric dust dynamics associated with the Siberian High and the westerly jet stream in NCA

Although dust emission from the dust sources in CA is also dependent on drought and relevant vegetation cover, type and soil moisture (Liu et al., 2020; Shi et al., 2021,2020; Xi and Sokolik, 2015a,b; Zhang et al., 2020), this review focuses on aeolian transport of dust, which is affected by the atmospheric circulation patterns and their dynamics. There are three major driving factors influencing modern dust mobility in CA (i) the Arctic and North Atlantic Oscillation (AO/NAO), (ii) the Siberian High and (iii) the Tibetan Plateau (Groll et al., 2013; Huang et al., 2011; Issanova et al., 2015; Kang et al., 2022; Shi et al., 2020). The NAO has a great influence on the climate in Europe and Asia during the cold season (Ogi et al., 2003), and the influence often extends southward to the Mediterranean (Dayan et al., 2008; Kaskaoutis et al., 2019; Papadimas et al., 2008). Cold air intrusion from north, northwest and northeast in CA caused by the western spur of the Siberian High leads to the dust activity in winter and spring (Orlovsky et al., 2005). The aloft Tibetan Plateau intensifies summer dust transport by thermodynamic forcing from sources in western CA and Taklimakan Desert (Kang et al., 2003; Lau et al., 2006).

The expanded Siberian High-pressure system can dominate winter and spring climate over Eurasia (Gong and Ho, 2002; Panagiotopoulos et al., 2005; Perşoiu et al., 2019; Sahsamanoglou et al., 1991). As stated above, dust storms in winter and spring over CA are linked to the western spur of the Siberian High (Issanova and Abuduwaili, 2017; Kang et al., 2022; Orlovsky et al., 2005), and the Siberian High has also been found to be one of the dynamic factors responsible for producing dust-storm events over the eastern Mediterranean, the Middle East and the northern Red Sea region (Labban et al., 2021, and references therein). Therefore, in consideration of the Siberian High permitting the dust-producing windstorms to occur (Roe, 2009), it is likely that the Siberian High system has exerted a significant influence on wind dynamics and loess deposition at least in Asia. Indeed, Dodonov and Baiguzina (1995) have suggested that the Asian high-pressure systems (e.g., the Siberian High) was regarded as the dominating dynamic for transporting coarse particles of loess deposits over the course of cold glacial periods in CA. Nevertheless, Machalett et al. (2008) demonstrated that the polar front has increased the frequency and strength of cyclonic storms and hence caused dust transport and loess accumulation along the Kyrgyz (northern) Tianshan piedmont. The polar front is a discontinuous border zone, generally separating the moister tropical air to the south from the drier and colder polar air to the north. However, the cold and dry polar air is most likely related to the cold air reservoir in Siberia (Serno et al., 2017). In this regard, loess accumulation during cold phases

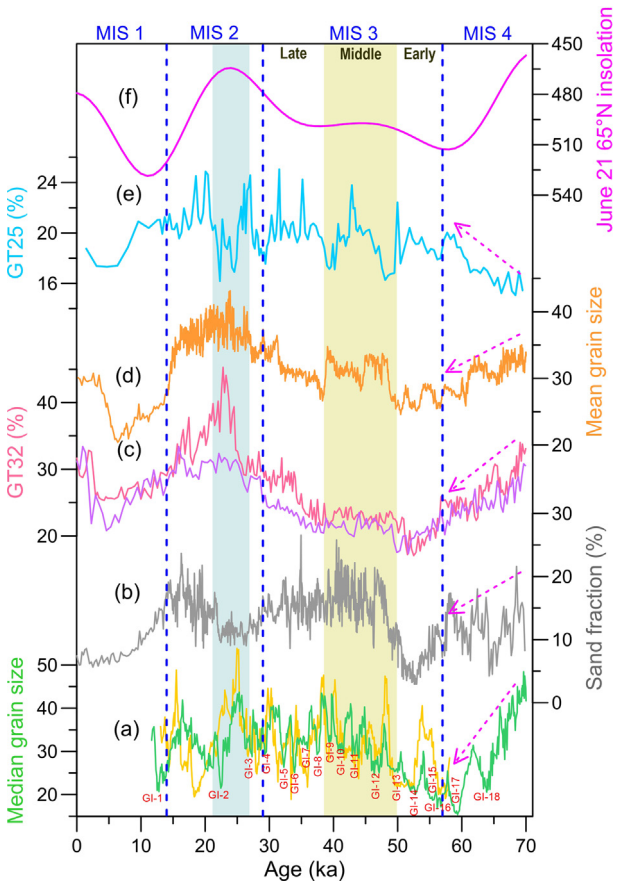

Fig. 4. Comparisons of proxy indicators of wind dynamics from northern and southern CA (a, b, e) and from the Chinese Loess Plateau (CLP) (c, d), and summer insolation at 65°N (Berger and Loutre, 1991) (f). (a) Median grain sizes of the Tacheng (green) and Yumin (yellow) loess section in the north of the Tianshan Mountains (Li et al., 2019c). (b) Sand fraction of the NLK loess section in eastern Ili Basin (Li et al., 2019b). (c) The contents of >32 μm fraction (GT32) in the Luochuan (purple) and Yimaguan (pink) loess taken in central CLP (Hao et al., 2012). (d) Mean grain sizes of the Jingyuan loess section located in the northwestern CLP (Sun et al., 2010). (e) The contents of >25 μm fraction (GT25) in the Darai Kalon section in the northeastern part of the Tajik Depression (Lu et al., 2020). The millennial-scale climate oscillations associated with Greenland interstadials (GI) were marked in (a). The MIS4 loess deposits are influenced by action of current scour (Li et al., 2019b), which most likely leads to various degree of modification of the original loess grain size distributions for the NLK section.

along the Kyrgyz (northern) Tianshan piedmont may also be attributed to the evolution of the Siberian High-pressure system.

We further evaluated the importance of Siberian High as the dynamic factor for the CA loess accumulation in the following. Grain-size analysis provides important information on depositional mechanisms and sedimentary environment of sediments (DiPietro et al., 2017). Increase in loess grain size in the Chinese Loess Plateau (CLP) is linked to a strengthened East Asian winter monsoon due to intensification of the Siberian High (Ding et al., 1995; Hao et al., 2012). Here, we used the contents of >32 μm fraction (GT32) in Luochuan and Yimaguan loess sections taken in central CLP (Hao et al., 2012) (Fig. 4c) and the high-resolution grain size record of the Jingyuan loess section located in the northwestern CLP (Sun et al., 2010) (Fig. 4d) to indicate intensity of the Siberian High. Grain size indexes from two well-dated loess sections were employed to reveal wind dynamics in NCA (Fig. 4a and b, Li et al., 2018a,2019c). The proxy indicators from NCA (Fig. 4a and b) and the CLP (Fig. 4c and d) during the last glacial are compared and similarities can be observed. Specifically, the increasing summer insolation (Fig. 4f) would result in rising summer temperature

during the MIS4, which went against reservoir of cold air in Siberia and shortens the presence of the cold air. Intensity of the Siberian High was thereby reduced, as revealed by the loess grain size records from the CLP (Fig. 4c and d). The pattern also holds for the loess grain size records in NCA (Fig. 4a and b), revealing reducing wind intensity therein. The relatively intensified Siberian High in the mid-MIS3 reflected by the grain size records of the CLP loess (Fig. 4c and d; grayish yellow box) has also caused wind dynamics to increase in NCA (Li et al., 2019b) (Fig. 4a and b). Minimum of the summer insolation has a counterpart of the significantly enhanced Siberian High during the Last Glacial Maximum (LGM) (Fig. 4c and d), which has strengthened the wind dynamics in NCA, as demonstrated by the increased median grain size of the Tacheng (green) and Yumin (yellow) loess section (Fig. 4a, bluish grey box). However, the sand fraction of the NLK section decreased during that time (Fig. 4b), in accordance with the reduced U-ratios (15.6–63.4 μm/5.61–15.6 μm) in the Remisowka loess section from the SE Kazakhstan (Machalett et al., 2008). Li et al. (2018a) and (2019b) attributed this to permafrost development in the Ili Basin during the LGM (Vandenberghe et al., 2014; Zhao et al., 2014), possibly influencing sediment supply. Hence, the reduced sand fraction did not imply weakened wind dynamics. By contrast, the increased sand fraction in the NLK section during the late MIS2 (Fig. 4b) corresponds to the increased median grain size of the Tacheng and Yumin loess sections (Fig. 4a), which was linked to the enhanced Siberian High. The late-MIS2 secondary peak are indeed observed on the CLP loess grain size curves (Fig. 4c and d). Consequently, the Siberian High-pressure system significantly influenced wind dynamics controlling dust variability in NCA. Grain size analyses of the quartz particles extracted from aeolian sediments (including loess deposits) from the Ili Basin, the northern Tianshan Mountains, and the Junggar Basin, also suggested that the Siberian High controlled the near-surface wind strength in northeastern arid CA during the Holocene (Gao et al., 2021). The region influenced by the Siberian High exhibit a fan-shaped pattern on spatial (Wang et al., 2018a), and NCA is situated at the western part of the region, suggesting that westward expansion of the Siberian High had an effect on climate regimes in NCA. In addition, dust activity in Aral Sea region was found to be linked to the Siberian High (Huang et al., 2011).

However, grain size records in the Darai Kalon section from Tajikistan (Lu et al., 2020) generally show opposite characteristics to those in NCA (Fig. 4). The contents of >25 μm fraction (GT25) in the Darai Kalon section display increasing trend during MIS4 (Fig. 4e). The mid-MIS3 has not witnessed marked increases in GT25, in contrast to the pattern in NCA. Importantly, the greatly diminished GT25 in the Darai Kalon section extremely differs from the sharp increases in loess grain sizes from East Asia and NCA during the LGM (Fig. 4). Since dust mobilization and deposition in Tajikistan mainly occurred in summertime (see 4.2 section), development of permafrost was not considered as the controlling factor for the reduced GT25 in the Darai Kalon section. Thus, these observations indicated that the wind regime for dust activity and loess accumulation was less influenced by the Siberian High-pressure system. The Siberian High is a shallow system in the Northern Hemisphere, and hence its expansion was probably restricted by the rough topography of the high Tianshan mountains (~7000 m) (Cohen et al., 2001). Therefore, the high mountain ranges have acted as a barrier to the influence of the Siberian High in SCA (e.g., Tajikistan), possibly precluding the influence of the Siberian High on wind dynamics and loess deposits therein.

In addition to loess grain size, sedimentation rate is often used to understand the relationship between atmospheric dust loading and climate changes in the past (Frechen and Dodonov, 1998; Li et al., 2020a; Sun and An, 2005; Újvári et al., 2017). Since dust emission efficiency (wind speed) and atmospheric transport can affect sedimentation rate variability (Maher et al., 2010; Újvári et al., 2017), sedimentation rate also facilitates unravelling the possible driving mechanisms of dust dynamics (Fitzsimmons et al., 2018; Kang et al., 2020; Kang et al., 2015; Lai et al., 2009; Sun and An, 2005).

To avoid the deficiency in the representability of a loess profile for understanding of variations in loess sedimentation rate, we compiled an extensive, although not exhaustive, database of previously published optically stimulated luminescence (OSL) ages of loess sections from the CLP, NCA, and Eastern/Central Europe (ECE) (Table S2, Fig. 5a, Table S3) according to several criteria. First and foremost, the collected luminescence ages must be peer-reviewed and published, which have been thoroughly analyzed and discussed in corresponding references (Table S2). Second, the selected loess sections should span nearly ~70 ka or at least ~60 ka for deciphering variations in dust concentrations on orbital timescales. For the interpretation of LGM dust variabilities, we collected luminescence ages of loess sections covering 19–26 ka from the above-mentioned three regions. Third, luminescence samples were collected from sections with roughly regular and relatively closely-spaced sampling depth intervals, and there should be at least one luminescence age in between 19 ka and 26 ka, with an estimated error not exceeding 2 ka. The luminescence ages/chronologies were used to estimate variation trends in loess sedimentation rate during the LGM. Consequently, 10 loess sections were compiled from the CLP, with 295 luminescence ages in total, 11 sections from the NCA, with 192 luminescence ages and 4 loess sections from the ECE with 110 luminescence ages. The OSL ages (Table S3) were subsequently used to calculate probability density functions (PDFs) for the CLP, NCA, and ECE, respectively (Fig. 5). An age cluster in a PDF plot is usually interpreted as a reflection of enhanced dust accumulation/activity and thus higher sedimentation rate (Kang et al., 2015; Lai et al., 2009; Singhvi et al., 2001; Yu and Lai, 2012). In this review, the OSL samples collected in roughly regular depth intervals rather than targeting key horizons, were only included in the dataset. Thus, the dataset is assumed to be largely unbiased (Singhvi et al., 2001), and age clusters indicate increased sedimentation rates.

For the last glaciation, the probability density curves for the OSL ages of loess sections from the CLP, the NCA and the ECE were shown in Fig. 5b–d. Notably, more rapid loess accumulation during the MIS3 than the MIS2 (Fig. 5c) verifies our previous conclusion (Li et al., 2019b), demonstrating influences of sediment recharge and supply in provenance related to moisture availability on loess sedimentation rate in the NCA, other than wind dynamics. That may partially explain the difference in probability density curve at ~70 ka between the CLP and the NCA (Li et al., 2019b). Therefore, much emphasis was put on changes in loess sedimentation rate during the LGM. Comparison of the probability density curves revealed accelerated dust accumulation during the LGM in the three regions (Fig. 5b–d). However, some differences could be distinguished in Fig. 5e–g. In particular, peaks of loess sedimentation rates for the CLP and the ECE occurred at ~20 ka and ~25 ka, respectively during the LGM (Fig. 5e and g), while loess sedimentation rates in the NCA were higher in the two periods (Fig. 5f, yellow boxes). On the one hand, this scenario further demonstrated that aeolian dynamics for dust mobilization and deposition in the NCA has been affected by the Siberian High (Aizen et al., 1997; Issanova and Abuduwaili, 2017; Li et al., 2018a; Li et al., 2019b; Small et al., 1999; Wu and Wang, 2002). The cold fronts associated with the Siberian High drew strong surface wind gusts close to the surface and produced near-surface convection, which was responsible for dust outbreaks (Roe, 2009, and references therein). Interactions between the westward expansion of the Siberian High and the near-surface westerlies also resulted in the vertical wind shear, increasing cyclonic activity and producing strong dust activity

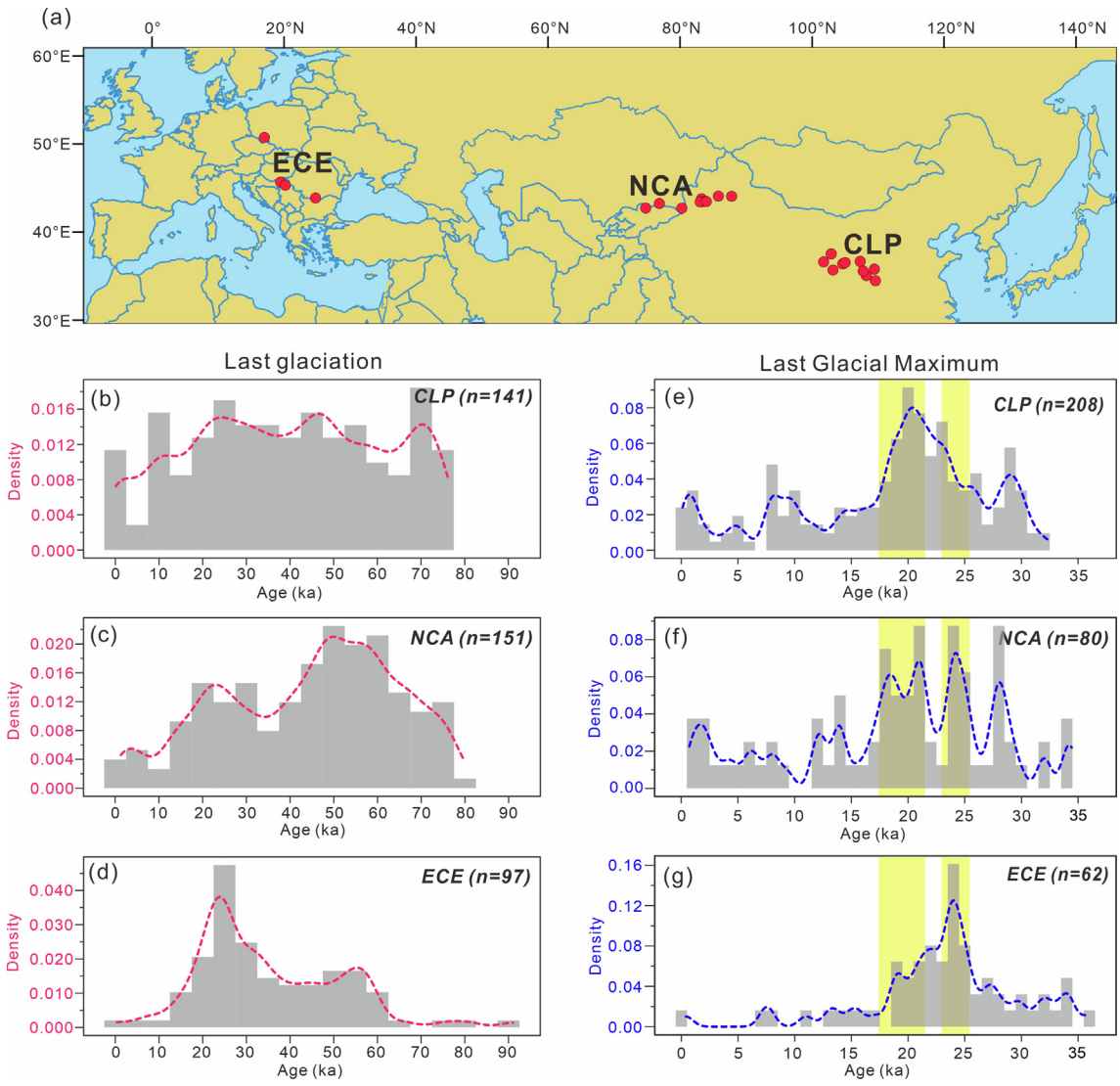

Fig. 5. Locations of loess sections (a) used in this review. See Table S2 for details of the loess sections and relevant references. Probability density plots (PDFs) for loess optically stimulated luminescence (OSL) ages over the Last glacial (b, c, d) and the Last Glacial Maximum (LGM) (e, f, g) from the CLP, the northern Central Asia (NCA) and the Eastern/Central Europe (ECE) (d).

(Shi et al., 2020). On the other hand, the coincident peaks in loess sedimentation rate at ~25 ka between the NCA and the ECE (Fig. 5f, g and Fig. 6a, b) implies that the atmospheric dynamic processes for the ECE loess accumulation also permitted the dust-producing windstorms to occur in the NCA.

The NAO/AO indices (Thompson and Wallace, 1998; Wu and Wang, 2002) largely control the climate in the Northern Hemisphere, especially during winter (Deser, 2000; Dickson et al., 2000). Numerical modeling results suggested that significant cooling in northern high latitudes could generate a low NAO index and a negative index of AO (Bond et al., 2001; Shindell et al., 2001; Sung et al., 2006). Temperature records from the NGRIP ice core indicated higher temperatures during the late-LGM (19–23.3 ka) relative to the early-LGM (23.3–26 ka) (Fig. 6c). Meanwhile, the North Atlantic Heinrich cold event H2 occurred in the early-LGM (Bond et al., 1992). Therefore, we claim that during the early-LGM, synoptic situations were very similar to negative phases of the NAO/AO and to positive phases during the late-LGM.

Alternatively, the benthic $\delta^{18}O$ (Lisiecki and Raymo, 2005), possibly representing fluctuations in North American ice volume (Clark and Pollard, 1998; Doughty et al., 2021), continuously increased during the LGM (Lisiecki and Raymo, 2005), which demonstrated the lower North American ice volume during the early-LGM than that during the late-LGM. Poleward-equatorward displacement of the North American Westerly Jet Stream reflected by loess-paleosol L^* index indicated the drastic advance of the Laurentide Ice Sheet during the late-LGM (Wang et al., 2021) (Fig. 6d). North American Ice Sheet reconstruction also showed largest ice volume in the late-LGM (Gowan et al., 2021) (Fig. 6e). Wang et al. (2021) suggested that under large North American Ice Sheets, equatorward displacement of the North American tropospheric Westerly Jet Stream produced positive AO mode in summers; inversely, poleward displacement of the North American tropospheric Westerly Jet Stream produced negative AO modes in summers, supporting our previous conclusion. In addition, the isotopic composition of 7H primarily recorded changes in the position of the North Atlantic storm track and associated changes of moisture advection to the Alps (Luetscher et al., 2015). Újvári et al. (2017) proposed that such large-scale atmospheric modulations are related to the predominant modes of NAO. During periods of dominant NAO– phase, the 7H Alpine stalagmite registered negative $\delta^{18}O$ excursions. In this context, the more depleted 7H $\delta^{18}O$ records

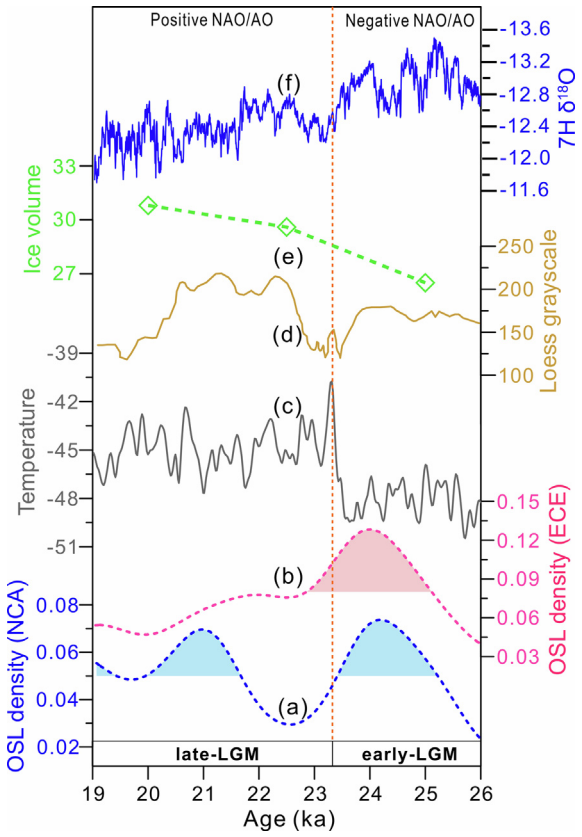

Fig. 6. Comparisons of proxy records during the LGM: PDF curves of loess OSL ages from the NCA (a) and ECE (b), NGRIP temperature reconstructed from atmospheric nitrogen isotope ratio (Kindler et al., 2014) (c), grayscale variations of the Keller Farm loess-paleosol record (Wang et al., 2021) (d), North American ice volumes (Gowan et al., 2021) (e), composite 7H stalagmite $\delta^{18}O$ record (Luetscher et al., 2015) (f).

during the early-LGM also indicated domination of the negative NAO modes (Fig. 6f).

More frequent Rossby-wave breaking associated with enhancement and southward migration of jet stream (Laine et al., 2009; Luetscher et al., 2015) led to a tendency toward more cyclone wave breaking and less anticyclonic wave breaking events (Laine et al., 2009; Pausata et al., 2011; Riviere et al., 2010). The higher cyclone density is thought to increase dustiness in both the winter and spring periods in dust-emitting regions of the ECE such as floodplains and outwash fans (Raible et al., 2007; Sima et al., 2013; Újvári et al., 2017). Since the NAO had a dynamic link to Rossby wave breaking events (Rivière and Orlanski, 2007), dust flux in the ECE was significantly related to NAO mode, and the dust minima (maxima) occurred during a persistent NAO+ (NAO−) phase with a more northerly (southerly) storm track (Újvári et al., 2017). As a result, a peak on the ECE PDF curve indicating increase in loess SR is observed in the early-LGM (Fig. 6b). This is supported by the abnormal dusty conditions in the central-east Mediterranean during March 2018 highly related with a negative NAO phase (Kaskaoutis et al., 2019). Simultaneously, additional wave breaking was possibly induced over CA and East Asia (Luetscher et al., 2015), triggering strong meridional advection patterns underneath upper-level jet excursions and generating dust storms over the regions. Dust emissions or dust storms have peaks in spring in the eastern and northern parts of CA (Nobakht et al., 2019; Nobakht et al., 2021). Therefore, occurrence of dust storms in NCA was likely influenced by frequency of the Rossby wave breaking events associated with the NAO mode during winter and spring. Several studies have shown that the winter NAO/AO directly affected the atmospheric conditions in CA (Aizen et al., 1997; Chen et al., 2008; Lan et al., 2021; Lan et al., 2020; Li et al., 2008; Small et al., 1999). Consequently, it is relevant to link the early-LGM peak on the NCA PDF curve (Fig. 6b) to impacts of the NAO mode.

We here exemplified the above view focusing on the north of the Tianshan Mountains. The NAO-phase, in response to the presence of the Fennoscandian ice shield during the LGM (Luetscher et al., 2015), made the Rossby-wave breaking events of jet stream more frequent over eastern Europe and CA (Fig. 7). In this context, the north of the Tianshan Mountains is located at a zone before ridge and after trough, where a high-pressure center appeared on the surface (Fig. 7). The wind field at 10 m AGL (above ground level) in spring, fall and winter for 1980–2016 in north of the Tianshan Mountains clearly shows a high-pressure center near the Balkhash Lake (Fig. 8a, b, d). Zhang et al. (2021) also indicated occurrence of the high-pressure center associated with westerly jets. Since the mean wind fields show that the center invariably stands in all seasons except for summer (Fig. 8a, b, d), we propose that the high pressure would be enhanced during negative NAO phase. The strengthened winds (blue dashed arrows in Fig. 8e–g) attributed to the enhanced high pressure probably led to

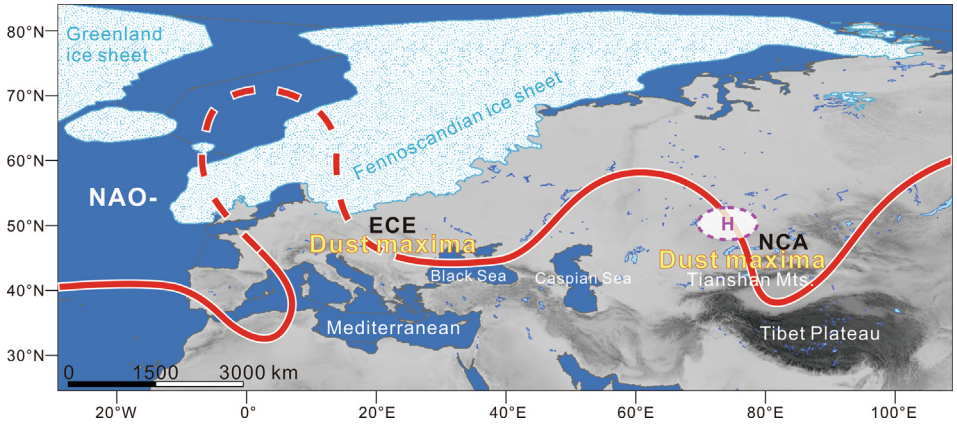

Fig. 7. A concept map showing that more frequent Rossby-wave breaking events of the jet stream over Western Europe during negative North Atlantic Oscillation phase induced more wave breaking events over CA through jet stream excursions (red line), which triggered dust-mobilizing storms in ECE and NCA. This map is modified after Luetscher et al. (2015). Red dashed line: meander of the Westerly jet stream; H: high pressure center.

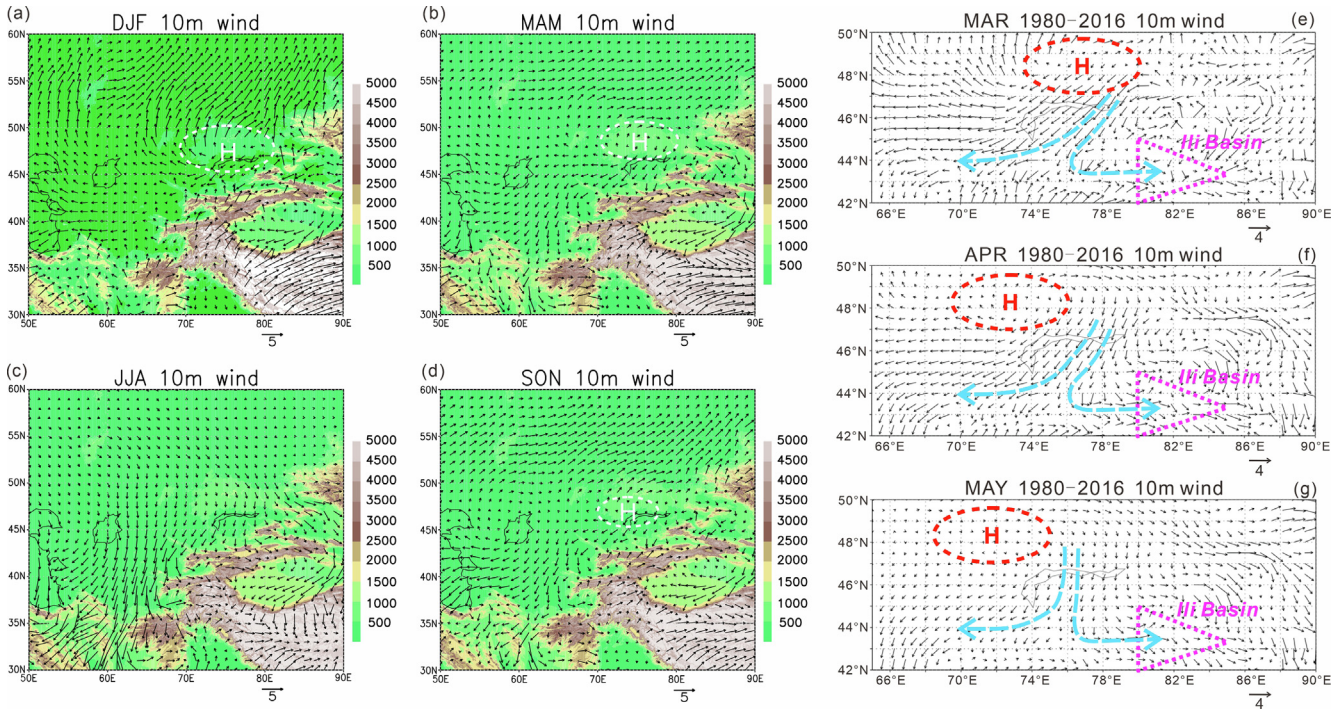

Fig. 8. (a–d) Map showing the mean wind fields at 10 m AGL (above ground level) in four seasons for 1980–2016 in CA. (e–g) The mean wind field at 10 m AGL in spring for 1980–2016 in north of the Tianshan Mountains. Data were extracted from the Modern-Era Retrospective analysis for Research and Applications, version 2 (MERRA-2) (Gelaro et al., 2017). The (e–g) is modified after Li et al. (2020c). H: high pressure center.

accelerated loess accumulation in the Ili Basin and southeastern Kazakhstan, yielding higher loess sedimentation rates.

In synopsis, in this sub-section we clarified the atmospheric dust dynamics over NCA, based on sedimentology proxy records of loess deposits. The Siberian High-pressure system and the NAO mode played the vital role in controlling dust mobilization and loess accumulation in NCA, and significance of the NAO mode in dust activity was recognized for the first time over the region according to the data of loess sedimentation rates. However, the Siberian High and the NAO mode may act as the major aeolian dust dynamics on the different timescales. Based on comparisons of indicators of wind dynamics (Fig. 4), the coupled relationships of variation trends between the dust dynamics in NCA and the Siberian High were valid at orbital time scales. Li et al. (2019b) suggested that the Eurasian ice volume during the MIS2 and MIS4, and the boreal summer insolation during MIS3 when the Eurasian ice volume decreased sharply, have forced changes in wind regimes in the Ili Basin, through their influences on the Siberian High at orbital scale. Therefore, the Siberian High may exert a huge influence on a long-term variation trend of dust dynamics. Újvári et al. (2017) have demonstrated that negative/positive NAO phase dominant periods coincided with Greenland stadial/interstadial, respectively. The operation of the NAO mode on dust dynamics was not only supported by the synchronously increased loess sedimentation rates during the early-LGM (or H2 cold event) shown by the age cluster in the PDF plot (Fig. 5e–g), but by a general Greenland stadial/interstadial pattern displayed by the NCA loess (Fig. 4a; Li et al., 2018a; Song et al., 2018). Thus, it implies that the remarkable short-term fluctuations of dust dynamics were closely correlated with the NAO modes. Therefore, the Siberian High was mainly responsible for driving orbital-scale variations in dust deposition; by contrast, the atmospheric dynamic processes on millennial timescales most likely responded to the NAO mode.

4.2. The Caspian Sea – Hindu Kush index (CasHKI) as dust dynamics for loess accumulation in SCA

Previous studies (Ding et al., 2002; Vandenberghe et al., 2006; Yang et al., 2006) supposed that loess deposition in southern Tajikistan was controlled by the regional westerly winds. However, recent study about element geochemistry of Tajikistan loess indicating the near-surface air currents from north and/or northwest argued against the previous assumption (Li et al., 2016b). Subsequently, Li et al. (2019a) and Li and Song (2021) compared the trace elements of loess deposits from the Ili Basin and the Afghan-Tajik Basin (Fig. 9a) to reveal their source characteristics. In comparison to the Ili loess, the Tajikistan loess differed from the upper continental crust (considered as a "sediment" with extensive sources and intensive mixing), and showed relatively identical elemental concentrations for different samples (Fig. 9a). That was regarded to indicate local and single sourcing, thus implying that large amounts of dust materials from Karakum Desert to the west were not transported to the Afghan-Tajik Basin albeit with their proximity (Li et al., 2019a). Therefore, the atmospheric circulation patterns responsible for dust activity in the Afghan-Tajik Basin was paid considerable attention (Li et al., 2019a; Tian et al., 2021).

The frequency bars computed from time series of the Total Ozone Mapping Spectrometer aerosol index reveal that dust activity maximizes from May to September in the Afghan-Tajik Basin due to nearly absence of precipitation, reduced soil moisture, higher near-surface wind speed, and relatively low vegetation cover (Fig. 9b), and the same occurs in nearly whole SCA region (Opp et al., 2017; Orlovsky and Indoitu, 2013; Rashki et al., 2018; Rupakheti et al., 2020) (Fig. 1b). The summer mean 850 hPa wind streamlines (ms^{-1}) primarily show northerly wind currents over CA, and are deflecting to westerlies within the Afghan-Tajik Basin (Fig. 10a). The deflecting winds are intimately related to dust

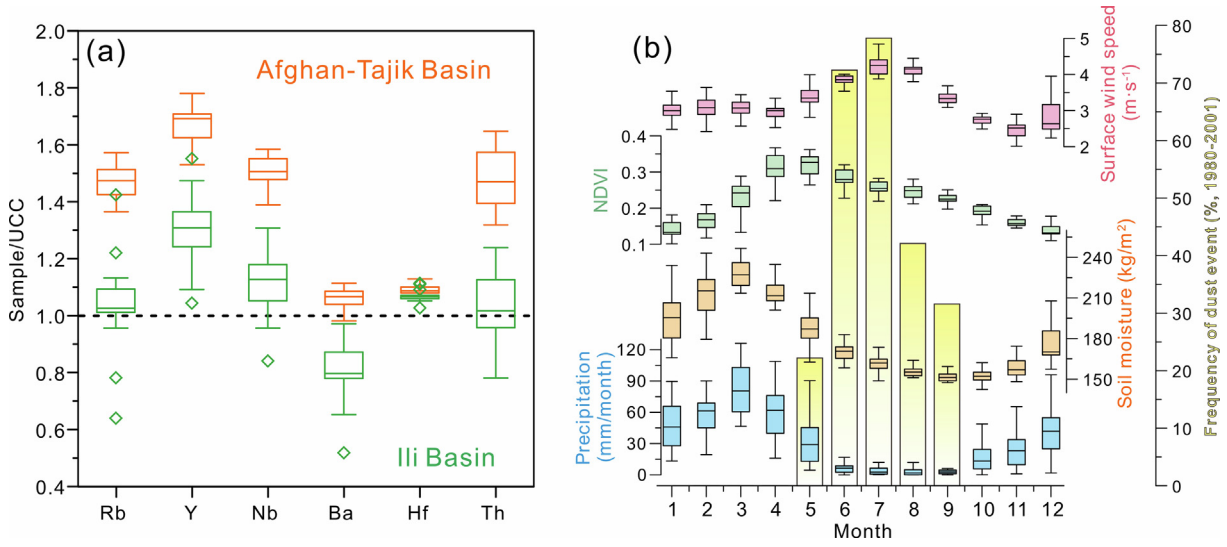

Fig. 9. (a) Box plot for the UCC-normalized ratios of stable trace elements and Zr of loess deposits from the Ili Basin and the Afghan-Tajik Basin (modified after Li and Song, 2021). UCC: upper continental crust. (b) Comparisons between monthly precipitation (1980–2001), soil moisture (1980–2001), Normalized Difference Vegetation Index (NDVI) (1982–2001), and surface wind speed (1980–2001) over the Afghan-Tajik Basin (36.7°–38.6°N, 67.3°–70°E). The bar charts illustrate the monthly frequency of occurrence of dust events defined by the Total Ozone Mapping Spectrometer aerosol index (TOMS-AI) (https://disc.sci.gsfc.nasa.gov/dataholdings/PIP/aerosol_index.shtml) during 1980–2001 (modified after Li et al., 2019a).

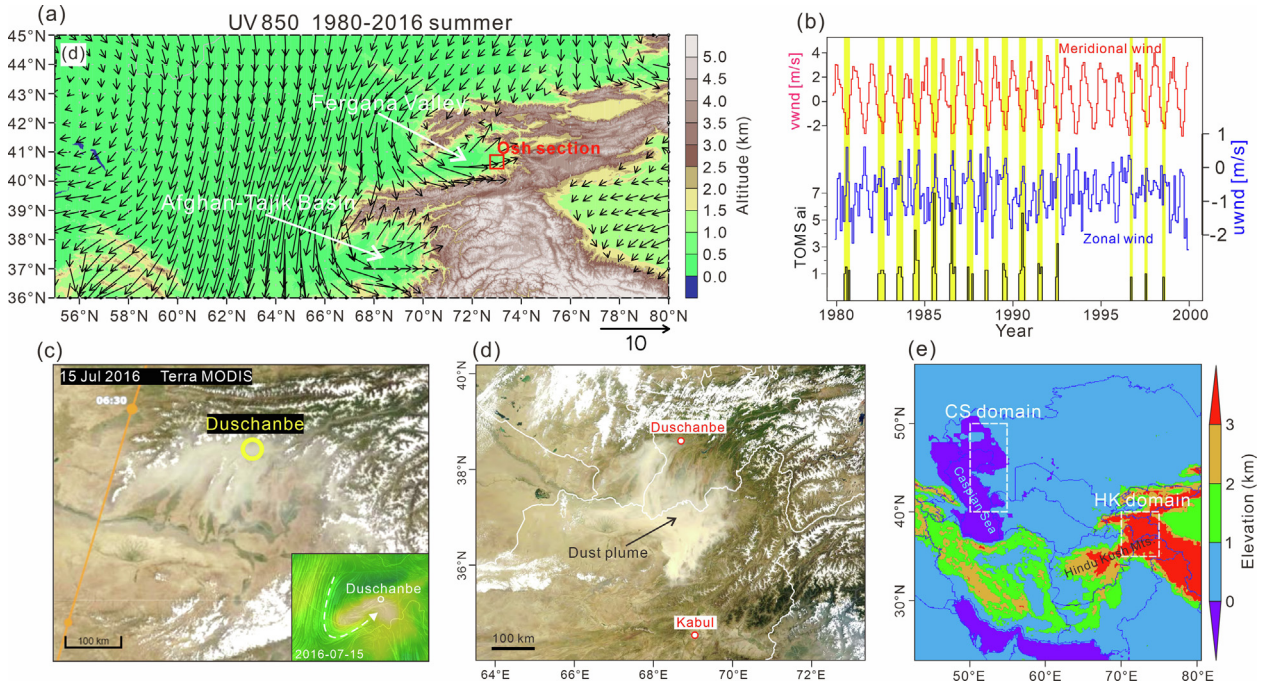

Fig. 10. (a) Summer mean 850-hPa vector winds (ms^{-1}) in CA for the years 1980–2016 [data from MERRA-2 (https://gmao.gsfc.nasa.gov/reanalysis/MERRA-2/), (Gelaro et al., 2017)]. (b) Time series of the monthly TOMS-AI (1980–2001, https://disc.sci.gsfc.nasa.gov/dataholdings/PIP/aerosol_index.shtml) and the zonal/meridional wind stress (1980–2000). (c) Satellite imagery (https://aeronet.gsfc.nasa.gov/) displaying a dust storm over the Afghan-Tajik Basin and the relevant atmospheric circulation pattern (https://earth.nullschool.net/) on July 15, 2016. (d) A dust storm developed over the Afghan-Tajik Basin on 25th June 2011 (http://earthobservatory.nasa.gov/) (Schettler et al., 2014). (e) Geomorphologic map with the locations of the Caspian Sea (CS) domain and the Hindu Kush (HK) domain.

outbreaks in the basin (Fig. 10b). A case study of a dust storm affecting the Afghan-Tajik Basin on 15 July 2016 (Fig. 10c) displayed a cyclonic circulation produced from the deflecting flows, which promoted dust emissions (Fig. 10c). The deflecting westerlies transported the dust eastward, which was then settled in western Pamirs (Fig. 10d), and the dust plume primarily originated from the interior of the basin, particularly the foothills in the northern Afghanistan (Li et al., 2019a). The proximal sources and short-distance aeolian transport thereby explained characteristics of the trace elements (Fig. 9a).

Kaskaoutis et al. (2015,2016) have tightly related the CasHKI to the dust activity over Central and southwest Asia, which was later verified by other studies (Hamidianpour et al., 2021; Kaskaoutis et al., 2018). The CasHKI was defined as the difference between the spatial-averaged mean sea-level pressure (MSLP) anomalies from the mean 1981–2010 climatology over the Caspian Sea

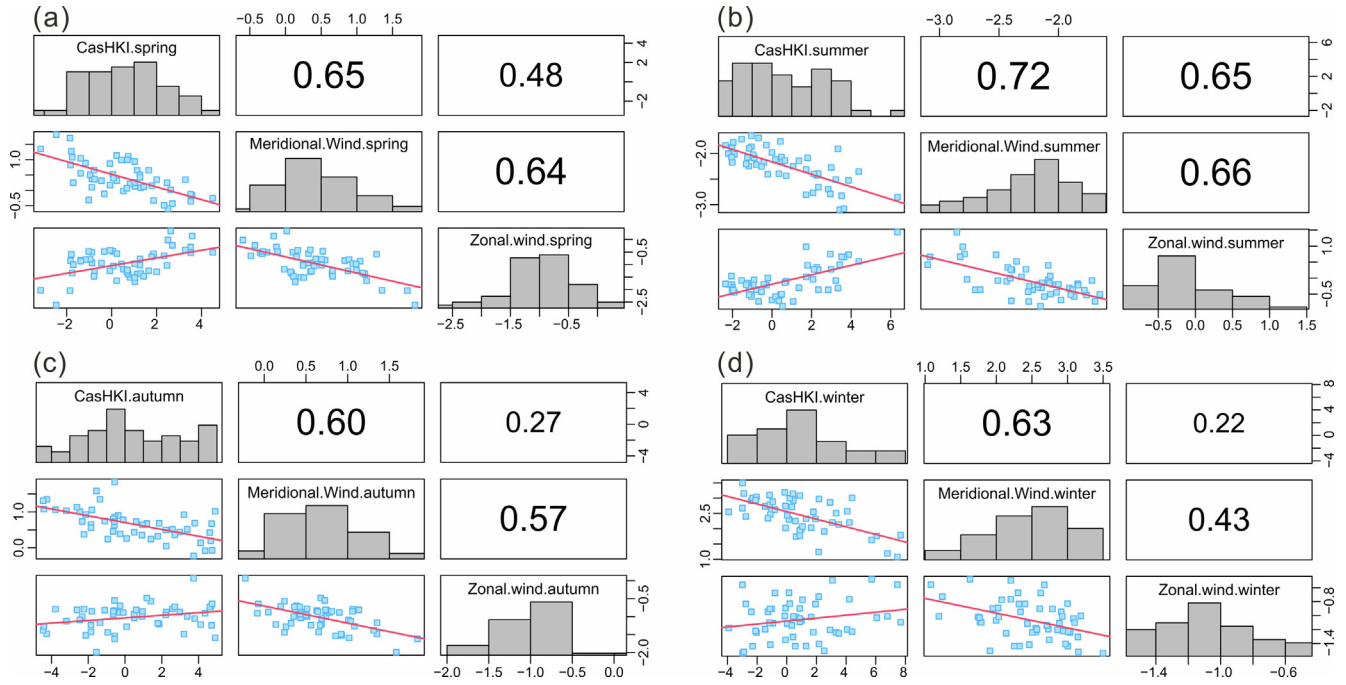

Fig. 11. Correlation analysis between the annual-means of the meridional and zonal wind speeds at Termez station with the Caspian Sea-Hindu Kush Index (CasHKI) values in spring (a), summer (b), autumn (c) and winter (d) during 1963–2014 (modified after Li et al., 2019a).

domain (40°–50°N, 50°–55°E) and Hindu Kush domain (35°–40°N, 70°–75°E), i.e., CasHKI = $MSLP_{anom.\_Caspian\ Sea} - MSLP_{anom.\_Hindu\ Kush}$. The high CasHKI values were found to be associated with significant increases in dust emission due to stronger winds and vice versa (Kaskaoutis et al., 2016,2017).

Since the Afghan-Tajik Basin basically lies within the Hindu Kush domain and is in the downwind direction of the northerlies and the deflecting westerlies (Fig. 10a), we examined the relation between the CasHKI intensity and the wind dynamics in the Afghan-Tajik Basin. The linear regression analysis (Fig. 11) revealed that the CasHKI values were strongly associated with the summer wind strength at Termez station located in the western Afghan-Tajik Basin, and the meridional and zonal wind (northerlies and westerlies, respectively) speeds exhibited higher correlation with CasHKI (R = 0.72 and 0.65) (Fig. 11b). Therefore, Li et al. (2019a) provided first evidence for control of the CasHKI on the aeolian processes in the basin. However, there are weaker correlations for other seasons, particularly for the zonal wind (Fig. 11a, c, d). Moreover, at several cases the meridional wind may be shifted to southerlies and the zonal component to exhibit weak easterlies (Fig. 11a, c, d) during the other seasons. Consequently, these lines of evidences strengthened the interpretations of the CasHKI largely controlling the summer dust mobilization in the Afghan-Tajik Basin. The positive CasHKI modes triggered the enhanced wind dynamics over the basin, which increased the probability of dust storms (Li et al., 2019a).

Although CasHKI variation and long-term trends have been proven to be highly associated with wind regime and dust activity in SCA and over southwest Asia from a series of previous publications (Kaskaoutis et al., 2018,2016,2017; Li et al., 2019a; Shi et al., 2020), the causes of variations in the CasHKI intensity have not yet been fully addressed, as well as its possible association with the large-scale climate systems (Kaskaoutis et al., 2018; Li et al., 2019a). On the decadal timescale, by comparisons of observation records, Lu et al. (2020) showed that relatively high CasHKI value were accompanied by a positive Siberian High index and a negative AO index, indicating their associations. While Kaskaoutis et al. (2017) stated that CasHKI values are strongly influenced by the Siberian High during winter and the Iranian ridge moving northward during summer. However, as yet, the physical mechanisms

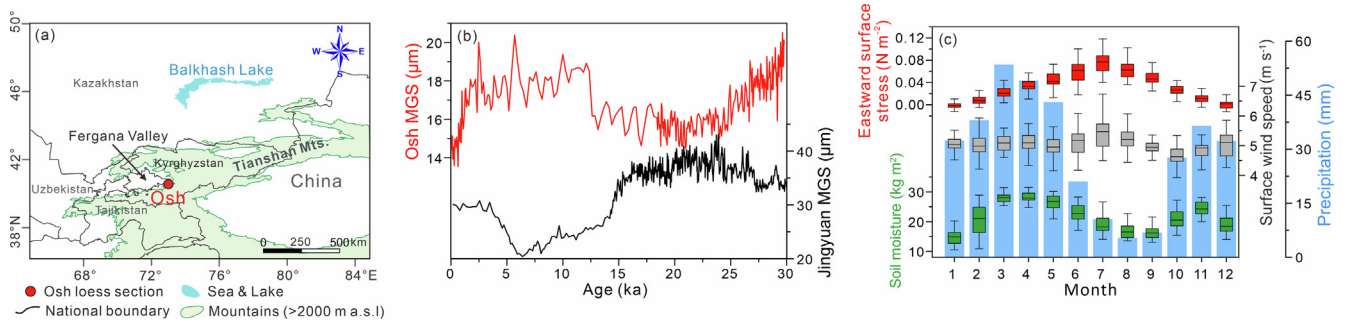

Fig. 12. (a) The locations of the Fergana Valley and the Osh loess section (red solid circle). (b) Comparisons of mean grain size (MGS) records between the Jingyuan loess section from the northwestern CLP (Sun et al., 2010) and the Osh section from the Fergana Valley (Li et al., 2021) since 30 ka. (c) Monthly comparisons between zonal wind stress and surface wind speed that were taken from the MERRA (https://gmao.gsfc.nasa.gov/reanalysis/MERRA/), soil moisture (data source: https://www.ecmwf.int/en/forecasts/datasets/reanalysis-datasets/era-interim) during 1980–2016, and precipitation recorded at Osh station during 1881–1997 (data source: https://www.ncdc.noaa.gov/data-access).

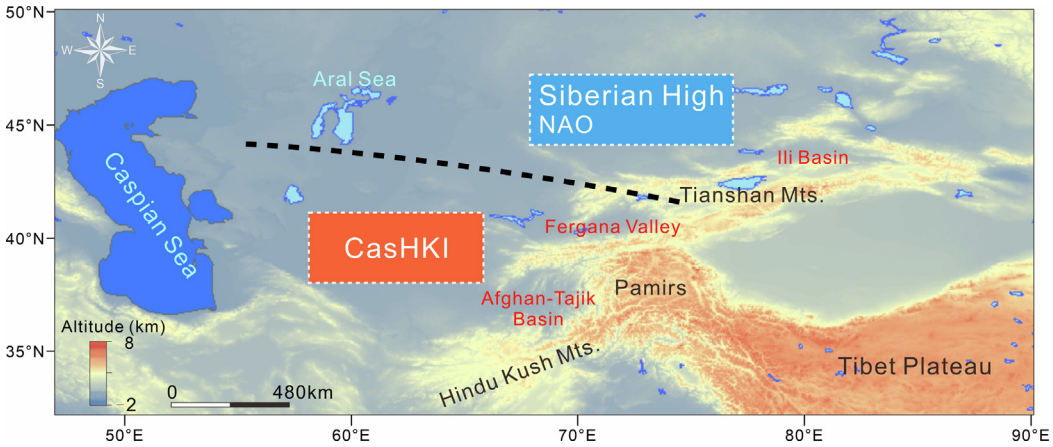

Fig. 13. Sketch map showing the different aeolian dynamics for loess deposition in the northern and southern part of CA. The black dashed line indicates the boundary between northern and southern CA regarding the atmospheric dust dynamics.

at play are far from being well understood. Subsequently, Li et al. (2021) speculated that the precession-related maximum North-Hemisphere seasonality might result in higher frequency of occurrence for high CasHKI modes. The precession-driven maximum seasonality (Kutzbach et al., 2014; Kutzbach et al., 2020) increased climate difference between winter and summer, which seemingly facilitated strengthening of the Siberian High and northward migration of the Iranian ridge synchronously, resulting in high-CasHKI modes. In this regard, it may be in accord with the statement of Kaskaoutis et al. (2017). Verification of these processes, however, require more research, including the analyses of loess-paleosol sequences in SCA.

5. A boundary of different atmospheric dust dynamics in CA: Insights from the Fergana loess deposits

In above sections, it is suggested that the aeolian dust dynamics were associated with the Siberian High and the NAO mode in NCA, while the dynamics in SCA (the Afghan-Tajik Basin) were mostly driven by the CasHKI mode. The boundary of these two dust-dynamics systems, however, remains largely unknown. This gap can be filled by investigating dust variability reflected by loess deposits at sites between NCA and SCA. Therefore, Li et al. (2021) took and analytically examined a loess section (named Osh section) from the Fergana Valley (Fig. 12a).

Based on investigations of the Osh loess grain sizes, past atmospheric dust dynamics in the valley was reconstructed (Li et al., 2021). Increase in mean grain size of the Jingyuan loess section in the northwestern CLP is linked to intensification of the Siberian High (Sun et al., 2010). A markedly negative correlation since 30 ka between the mean grain sizes of the Osh loess and the Jingyuan loess (Fig. 12b) thereby suggested that the Siberian High did not significantly affect wind dynamics at the Osh site (Li et al., 2021). Although the Siberian High controls the winter and spring climate over Eurasia (Ding and Krishnamurti, 1987; Gong and Ho, 2002; Panagiotopoulos et al., 2005), expansion of the Siberian High to the south is restricted by the elevated Tianshan mountains due to its shallowness (Cohen et al., 2001). As a result, the Fergana Valley was not exposed to effects of the Siberian High (Li et al., 2021). In winter periods with positive anomalies and strengthening of the Siberian High, an enhancement of the northeastern flow occurred over CA (Perşoiu et al., 2019), which contributed little to the dust emissions in the valley. Therefore, range of influence of the Siberian High did not expand beyond the Fergana Valley in terms of loess deposition in CA. On the other hand, the decreased precipitation and soil moisture, and the relatively increased surface wind speed during summer-time (Fig. 12c) facilitate wind erosion and dust mobilization (Li et al., 2021), making dust activity over the Fergana Valley maximize during the hot and dry summer, in agreement with the case in the Afghan-Tajik Basin. The summer atmospheric circulation pattern in the Fergana Valley also shows strong similarity to that in the Afghan-Tajik Basin (Fig. 10a). Therefore, given location of the valley near the Hindu Kush domain, Li et al. (2021) supposed that the dust dynamics in the valley likely depend on the CasHKI intensity.

In summary, the main factor that influences the atmospheric dust dynamics in the Fergana Valley differs from those in NCA, and the CasHKI intensity has possibly affected the loess deposition in the valley. The boundary of different atmospheric dust dynamics in between NCA and SCA is approximately in the north of the Fergana Valley. However, accurate determination of the boundary could benefit from investigations of aeolian dust dynamics in the Tashkent region based on loess deposits (Lazarenko et al., 1981; Smalley et al., 2006; Zhou et al., 1995).

6. Conclusions

Atmospheric dust dynamics for loess deposition in CA, which has received only limited attention till now, provides a better understanding of the linkages between climate variability and loess-paleosol sequence, and in parallel, strengthens the physical basis for paleoclimate reconstruction using loess sediments. This work provided an overview of the atmospheric dynamics affecting the dust sedimentation and loess deposits in CA. With investigations of trace element geochemistry, loess deposits from piedmonts of the CA mountains have been found to be dominated by proximal sources, and overall, they are of different origins in the north and south parts of the Tianshan Mountains. Such a provenance feature was associated with aeolian dust dynamics, other than the CA topography. The comparisons of grain size data of loess sedimentary sequences from the CLP, NCA and SCA supported the argument that the Siberian High-pressure system played the vital role in controlling dust mobilization and loess accumulation in NCA, whereas it was not the atmospheric-dynamic processes responsible for loess deposition in SCA. The significance of the NAO mode in dust activity was also recognized over NCA based on the LGM loess sedimentation rates and millennial-scale fluctuations in the loess records. More frequent Rossby-wave breaking events of jet stream during negative NAO phase over NCA enhanced the anticyclone center in the north of the Tianshan Mountains, which probably led to accelerated loess accumulation in the Ili Basin and southeastern Kazakhstan and yielded higher

loess sedimentation rates. We also tried to link the dust activity maximizing in summer in the Afghan-Tajikistan Basin (in SCA) to the CasHKI variability, a recently proposed index defined by the difference between the mean sea-level pressure anomalies over domains near the Caspian Sea and Hindu Kush. Higher CasHKI values have led to stronger transport and accumulation of dust in SCA. However, the mechanisms driving the CasHKI variability and the degree that this index may be involved in paleoclimatology studies constitute a real challenge for future research.

The Fergana Valley was selected as a potential transition zone between the aeolian dynamic systems in NCA and SCA. The grain size data of loess deposits, combined with meteorological and climatic data, suggested that the CasHKI phases also influenced the wind dynamics for dust mobilization in the valley. Therefore, the suggestion is to divide the CA region into two parts regarding atmospheric dynamics for aeolian dust, with a boundary extending from the North Tianshan Mountains to the southern Aral Sea (black dashed line in Fig. 13). In the northern part, dust emission mainly occurred in winter and spring (Nobakht et al., 2019,2021), and the Siberian High and the NAO phase constituted the major factors exerting a huge influence on dust activity and loess accumulation. By contrast, in the southern part, dust entrainment and deposition maximized in summer (Nobakht et al., 2019,2021), and were highly determined by the intensity of CasHKI. However, further study on the Tashkent loess would provide a valuable basis for improving precision of this division. In addition, the physical connections between the mid-latitude Westerlies and dust dynamics for loess deposition in CA still remain to be further explored up to now despite of the preliminary results shown in this review and from Li et al. (2021). Consequently, to ascertain the dynamic processes linked to the mid-latitude Westerlies that drive changes in aeolian loess deposition in CA is our specific recommendation for future critical research topic.

Declaration of Competing Interest

The authors declare that they have no known competing financial interests or personal relationships that could have appeared to influence the work reported in this paper.

Acknowledgements

This work was supported by the Second Tibetan Plateau Scientific Expedition and Research program (STEP) [grant number: 2019QZKK0101], the Natural Science Foundation of China [grant numbers: 42102238, 41977385], the Strategic Priority Research Program of Chinese Academy of Sciences (CAS) (grant numbers: XDB40000000, XDB26000000), Key Laboratory of Desert and Desertification, CAS [grant number: KLDD-2020-009], and the project of Special Research Assistant, CAS. D.G.K. acknowledges the project "PANhellenic infrastructure for Atmospheric Composition and climatE change" (MIS 5021516), which is implemented under the Action "Reinforcement of the Research and Innovation Infrastructure", funded by the Operational Programme "Competitiveness, Entrepreneurship and Innovation" (NSRF 2014-2020) and co-financed by Greece and the European Union (European Regional Development Fund). The authors thank Dr. Heng Liu from Xi'an Institute for Innovative Earth Environment Research for his help in plotting.

Appendix A. Supplementary material

Supplementary data to this article can be found online at https://doi.org/10.1016/j.gr.2022.04.019.

References

Aizen, V.B., Aizen, E.M., Melack, J.M., Dozier, J., 1997. Climatic and hydrologic changes in the Tien Shan, Central Asia. J. Clim. 10 (6), 1393–1404.
Berger, A., Loutre, M.F., 1991. Insolation values for the climate of the last 10 million years. Quat. Sci. Rev. 10 (4), 297–317.
Bond, G., Heinrich, H., Broecker, W., Labeyrie, L., McManus, J., Andrews, J., Huon, S., Jantschik, R., Clasen, S., Simet, C., Tedesco, K., Klas, M., Bonani, G., Ivy, S., 1992. Evidence for massive discharges of icebergs into the North Atlantic ocean during the last glacial period. Nature 360 (6401), 245–249.
Bond, G., Kromer, B., Beer, J., Muscheler, R., Evans, M.N., Showers, W., Hoffmann, S., Lotti-Bond, R., Hajdas, I., Bonani, G., 2001. Persistent solar influence on North Atlantic climate during the Holocene. Science 294 (5549), 2130–2136.
Chen, F., Yu, Z., Yang, M., Ito, E., Wang, S., Madsen, D.B., Huang, X., Zhao, Y., Sato, T., John B. Birks, H., Boomer, I., Chen, J., An, C., Wünnemann, B., 2008. Holocene moisture evolution in arid central Asia and its out-of-phase relationship with Asian monsoon history. Quat. Sci. Rev. 27 (3–4), 351–364.
Clark, P.U., Pollard, D., 1998. Origin of the middle Pleistocene transition by ice sheet erosion of regolith. Paleoceanography 13 (1), 1–9.
Cohen, J., Saito, K., Entekhabi, D., 2001. The role of the Siberian high in Northern Hemisphere climate variability. Geophys. Res. Lett. 28 (2), 299–302.
Dayan, U., Ziv, B., Shoob, T., Enzel, Y., 2008. Suspended dust over southeastern Mediterranean and its relation to atmospheric circulations. Int. J. Climatol. 28 (7), 915–924.
Dee, D.P., Uppala, S.M., Simmons, A.J., Berrisford, P., Poli, P., Kobayashi, S., Andrae, U., Balmaseda, M.A., Balsamo, G., Bauer, P., Bechtold, P., Beljaars, A.C.M., van de Berg, L., Bidlot, J., Bormann, N., Delsol, C., Dragani, R., Fuentes, M., Geer, A.J., Haimberger, L., Healy, S.B., Hersbach, H., Hólm, E.V., Isaksen, L., Kållberg, P., Köhler, M., Matricardi, M., McNally, A.P., Monge-Sanz, B.M., Morcrette, J.-J., Park, B.-K., Peubey, C., de Rosnay, P., Tavolato, C., Thépaut, J.-N., Vitart, F., 2011. The ERA-Interim reanalysis: Configuration and performance of the data assimilation system. Q. J. Roy. Meteorol. Soc. 137 (656), 553–597.
Deser, C., 2000. On the teleconnectivity of the "Arctic Oscillation". Geophys. Res. Lett. 27 (6), 779–782.
Dickson, R.R., Osborn, T.J., Hurrell, J.W., Meincke, J., Blindheim, J., Adlandsvik, B., Vinje, T., Alekseev, G., Maslowski, W., 2000. The Arctic Ocean response to the North Atlantic oscillation. J. Clim. 13 (15), 2671–2696.
Ding, Y., Krishnamurti, T.N., 1987. Heat-budget of the Siberian high and the winter monsoon. Mon. Weather. Rev. 115 (10), 2428–2449.
Ding, Z., Liu, T., Rutter, N.W., Yu, Z., Guo, Z., Zhu, R., 1995. Ice-volume forcing of East Asian winter monsoon variations in the past 800,000 years. Quat. Res. 44 (2), 149–159.
Ding, Z.L., Ranov, V., Yang, S.L., Finaev, A., Han, J.M., Wang, G.A., 2002. The loess record in southern Tajikistan and correlation with Chinese loess. Earth Planet. Sci. Lett. 200 (3–4), 387–400.
DiPietro, L.M., Driese, S.G., Nelson, T.W., Harvill, J.L., 2017. Variations in late Quaternary wind intensity from grain-size partitioning of loess deposits in the Nenana River Valley. Alaska. Quat. Res. 87 (2), 258–274.
Dodonov, A.E., 1991. Loess of Central Asia. GeoJournal 24, 185–194.
Dodonov, A.E., Baiguzina, L.L., 1995. Loess stratigraphy of Central Asia: palaeoclimatic and palaeoenvironmental aspects. Quat. Sci. Rev. 14 (7–8), 707–720.
Dong, W.H., Lin, Y.L., Wright, J.S., Xie, Y.Y., Ming, Y., Zhang, H., Chen, R.S., Chen, Y.N., Xu, F.H., Lin, N.M., Yu, C.Q., Zhang, B., Jin, S., Yang, K., Li, Z.Q., Guo, J.P., Wang, L., Lin, G.H., 2018. Regional disparities in warm season rainfall changes over arid eastern-central Asia. Sci. Rep. 8, 13051.
Doughty, A.M., Kaplan, M.R., Peltier, C., Barker, S., 2021. A maximum in global glacier extent during MIS 4. Quat. Sci. Rev. 261, 106948.
Engelbrecht, J.P., Derbyshire, E., 2010. Airborne Mineral Dust. Elements 6 (4), 241–246.
Engelstaedter, S., Tegen, I., Washington, R., 2006. North African dust emissions and transport. Earth-Sci. Rev. 79 (1–2), 73–100.
Fan, Y., Jia, J., Xia, D., Meadows, M., Wang, Z., 2021. Seasonality of response to millennial-scale climate events of the last glacial: evidence from loess records over mid-latitude Asia. Geochem. Geophys. Geosyst. 22. e2021GC009903.
Fitzsimmons, K.E., Nowatzki, M., Dave, A.K., Harder, H., 2020. Intersections between wind regimes, topography and sediment supply: perspectives from aeolian landforms in Central Asia. Palaeog. Palaeoclimatol. Palaeoecol. 540, 109531.
Fitzsimmons, K.E., Sprafke, T., Zielhofer, C., Gunter, C., Deom, J.M., Sala, R., Iovita, R., 2018. Loess accumulation in the Tian Shan piedmont: implications for palaeoenvironmental change in arid Central Asia. Quat. Int. 469, 30–43.
Frechen, M., Dodonov, A.E., 1998. Loess chronology of the Middle and Upper Pleistocene in Tadjikistan. Geol. Rundsch. 87 (1), 2–20.
Gao, F., Zheng, X., Jia, J., Li, K., Xia, D., Yang, J., Lu, H., Shi, F., Chen, Z., Wang, S., 2021. Evolution of near-surface wind strength in northeastern arid central Asia during the holocene. Paleoceanogr. Paleocl. 36. e2020PA003970.
Ge, Y., Abuduwaili, J., Ma, L., Liu, D., 2016. Temporal variability and potential diffusion characteristics of dust aerosol originating from the Aral Sea basin, central Asia. Water Air Soil Pollut. 227, 63.
Gelaro, R., McCarty, W., Suárez, M.J., Todling, R., Molod, A., Takacs, L., Randles, C.A., Darmenov, A., Bosilovich, M.G., Reichle, R., Wargan, K., Coy, L., Cullather, R., Draper, C., Akella, S., Buchard, V., Conaty, A., da Silva, A.M., Gu, W., Kim, G.-K., Koster, R., Lucchesi, R., Merkova, D., Nielsen, J.E., Partyka, G., Pawson, S., Putman, W., Rienecker, M., Schubert, S.D., Sienkiewicz, M., Zhao, B., 2017. The Modern-

Era Retrospective Analysis for Research and Applications, Version 2 (MERRA-2). J. Clim. 30 (14), 5419–5454.
Gholami, H., Mohammadifar, A., Malakooti, H., Esmaeilpour, Y., Golzari, S., Mohammadi, F., Li, Y., Song, Y., Kaskaoutis, D.G., Fitzsimmons, K.E., Collins, A. L., 2021. Integrated modelling for mapping spatial sources of dust in central Asia-An important dust source in the global atmospheric system. Atmos. Pollut. Res. 12 (9), 101173.
Gintzburger, G., Le Houérou, H.N., Toderich, K.N., 2005. The steppes of Middle Asia: post-1991 agricultural and rangeland adjustment. Arid. Land. Res. Manag. 19 (3), 215–239.
Gong, D.-Y., Ho, C.-H., 2002. The Siberian High and climate change over middle to high latitude Asia. Theor. Appl. Climatol. 72 (1-2), 1–9.
Goudie, A.S., 2014. Desert dust and human health disorders. Environ. Int. 63, 101–113.
Gowan, E.J., Zhang, X., Khosravi, S., Rovere, A., Stocchi, P., Hughes, A.L., Gyllencreutz, R., Mangerud, J., Svendsen, J.-I., Lohmann, G., 2021. A new global ice sheet reconstruction for the past 80 000 years. Nat. Commun. 12, 1–9.
Groll, M., Opp, C., Aslanov, I., 2013. Spatial and temporal distribution of the dust deposition in Central Asia – results from a long term monitoring program. Aeolian Res. 9, 49–62.
Guan, X., Yang, L., Zhang, Y., Li, J., 2019. Spatial distribution, temporal variation, and transport characteristics of atmospheric water vapor over Central Asia and the arid region of China. Global Planet. Change 172, 159–178.
Hamidianpour, M., Jahanshahi, S.M.A., Kaskaoutis, D.G., Rashki, A., Nastos, P.G., 2021. Climatology of the Sistan Levar wind: atmospheric dynamics driving its onset, duration and withdrawal. Atmos. Res. 260, 105711.
Hamzeh, M.A., Gharaie, M.H.M., Lahijani, H.A.K., Djamali, M., Harami, R.M., Beni, A. N., 2016. Holocene hydrological changes in SE Iran, a key region between Indian summer monsoon and Mediterranean winter precipitation zones, as revealed from a lacustrine sequence from Lake Hamoun. Quat. Int. 408, 25–39.
Hao, Q., Wang, L., Oldfield, F., Peng, S., Qin, L.i., Song, Y., Xu, B., Qiao, Y., Bloemendal, J., Guo, Z., 2012. Delayed build-up of Arctic ice sheets during 400,000-year minima in insolation variability. Nature 490 (7420), 393–396.
Huang, X., Oberhänsli, H., von Suchodoletz, H., Sorrel, P., 2011. Dust deposition in the Aral Sea: implications for changes in atmospheric circulation in central Asia during the past 2000 years. Quat. Sci. Rev. 30 (25–26), 3661–3674.
Indoitu, R., Kozhoridze, G., Batyrbaeva, M., Vitkovskaya, I., Orlovsky, N., Blumberg, D.G., Orlovsky, L., 2015. Dust emission and environmental changes in the dried bottom of the Aral Sea. Aeolian Res. 17, 101–115.
Indoitu, R., Orlovsky, L., Orlovsky, N., 2012. Dust storms in Central Asia: spatial and temporal variations. J. Arid Environ. 85, 62–70.
Issanova, G., Abuduwaili, J., 2017. Aeolian processes as dust storms in the deserts of central Asia and Kazakhstan. In: Förstner, U., Rulkens, W.H., Salomons, W. (Eds.), Environmental Science and Engineering. Springer, Singapore.
Issanova, G., Abuduwaili, J., Galayeva, O., Semenov, O., Bazarbayeva, T., 2015. Aeolian transportation of sand and dust in the Aral Sea region. Int. J. Environ. Sci. Technol. 12 (10), 3213–3224.
Jia, J., Wang, N., Wang, Z., Wang, S., Meadows, M., Wang, L., Fan, Y., Chen, J., 2022. Weakened dust activity in southern Central Asia during Heinrich events. Palaeogeog. Palaeoclimatol. Palaeoecol. 587, 110805.
Kang, S., Du, J., Wang, N., Dong, J., Wang, D., Wang, X., Qiang, X., Song, Y., 2020. Early Holocene weakening and mid-to late Holocene strengthening of the East Asian winter monsoon. Geology 48, 1043–1047.
Kang, S., Mayewski, P.A., Yan, Y., Qin, D., Yao, T., Ren, J., 2003. Dust records from three ice cores: relationships to spring atmospheric circulation over the Northern Hemisphere. Atmos. Environ. 37 (34), 4823–4835.
Kang, S., Roberts, H.M., Wang, X., An, Z., Wang, M., 2015. Mass accumulation rate changes in Chinese loess during MIS 2, and asynchrony with records from Greenland ice cores and North Pacific Ocean sediments during the Last Glacial Maximum. Aeolian Res. 19, 251–258.
Kang, S., Wang, X., Wang, N., Song, Y., Wang, D., Peng, J., 2022. Siberian High Modulated Suborbital-scale Dust Accumulation Changes over the Past 30 ka in the Eastern Yili Basin, Central Asia. Paleoceanography and Paleoclimatology. https://doi.org/10.1029/2021PA004360. In press e2021PA004360.
Kaskaoutis, D., Dumka, U., Rashki, A., Psiloglou, B., Gavriil, A., Mofidi, A., Petrinoli, K., Karagiannis, D., Kambezidis, H., 2019. Analysis of intense dust storms over the eastern Mediterranean in March 2018: impact on radiative forcing and Athens air quality. Atmos. Environ. 209, 23–39.
Kaskaoutis, D.G., Houssos, E.E., Minvielle, F., Rashki, A., Chiapello, I., Dumka, U.C., Legrand, M., 2018. Long-term variability and trends in the Caspian Sea – Hindu Kush index: influence on atmospheric circulation patterns, temperature and rainfall over the Middle East and Southwest Asia. Global Planet. Change 169, 16–33.
Kaskaoutis, D.G., Houssos, E.E., Rashki, A., Francois, P., Legrand, M., Goto, D., Bartzokas, A., Kambezidis, H.D., Takemura, T., 2016. The Caspian Sea-Hindu Kush Index (CasHKI): a regulatory factor for dust activity over southwest Asia. Global Planet. Change 137, 10–23.
Kaskaoutis, D.G., Rashki, A., Houssos, E.E., Legrand, M., Francois, P., Bartzokas, A., Kambezidis, H.D., Dumka, U.C., Goto, D., Takemura, T., 2017. Assessment of changes in atmospheric dynamics and dust activity over southwest Asia using the Caspian Sea-Hindu Kush Index. Int. J. Climatol. 37, 1013–1034.
Kaskaoutis, D.G., Rashki, A., Houssos, E.E., Mofidi, A., Goto, D., Bartzokas, A., Francois, P., Legrand, M., 2015. Meteorological aspects associated with dust storms in the Sistan region, southeastern Iran. Clim. Dyn. 45 (1–2), 407–424.
Kindler, P., Guillevic, M., Baumgartner, M., Schwander, J., Landais, A., Leuenberger, M., 2014. Temperature reconstruction from 10 to 120 kyr b2k from the NGRIP ice core. Clim. Past. 10, 887–902.
Kutzbach, J.E., Chen, G., Cheng, H., Edwards, R.L., Liu, Z., 2014. Potential role of winter rainfall in explaining increased moisture in the Mediterranean and Middle East during periods of maximum orbitally-forced insolation seasonality. Clim. Dyn. 42 (3–4), 1079–1095.
Kutzbach, J.E., Guan, J., He, F., Cohen, A.S., Orland, I.J., Chen, G., 2020. African climate response to orbital and glacial forcing in 140,000-y simulation with implications for early modern human environments. Proc. Nat. Acad. Sci. 117 (5), 2255–2264.
Labban, A.H., Mashat, A.-W., Awad, A.M., 2021. The variability of the Siberian high ridge over the Middle East. Int. J. Climatol. 41 (1), 104–130.
Lai, ZhongPing, Kaiser, K., Brückner, H., 2009. Luminescence-dated aeolian deposits of late Quaternary age in the southern Tibetan Plateau and their implications for landscape history. Quat. Res. 72 (3), 421–430.
Laine, A., Kageyama, M., Salas-Mélia, D., Voldoire, A., Rivière, G., Ramstein, G., Planton, S., Tyteca, S., Peterschmitt, J.Y., 2009. Northern hemisphere storm tracks during the last glacial maximum in the PMIP2 ocean-atmosphere coupled models: energetic study, seasonal cycle, precipitation. Clim. Dyn. 32 (5), 593–614.
Lan, J., Wang, T., Dong, J., Kang, S., Cheng, P., Zhou, K., Liu, X., Wang, Y., Ma, L.e., 2021. The influence of ice sheet and solar insolation on Holocene moisture evolution in northern Central Asia. Earth Sci. Rev. 217, 103645.
Lan, J., Zhang, J., Cheng, P., Ma, X., Ai, L.i., Chawchai, S., Zhou, K., Wang, T., Yu, K., Sheng, E., Kang, S., Zang, J., Yan, D., Wang, Y., Tan, L., Xu, H., 2020. Late Holocene hydroclimatic variation in central Asia and its response to mid-latitude Westerlies and solar irradiance. Quat. Sci. Rev. 238, 106330.
Lau, K.M., Kim, M.K., Kim, K.M., 2006. Asian summer monsoon anomalies induced by aerosol direct forcing: the role of the Tibetan Plateau. Clim. Dyn. 26 (7–8), 855–864.
Lazarenko, A.A., Bolikhovskaya, N.S., Semenov, V.V., 1981. An attempt at a detailed stratigraphic subdivision of the loess association of the Tashkent region. Int. Geol. Rev. 23 (11), 1335–1346.
Li, G., Yang, H.e., Stevens, T., Zhang, X., Zhang, H., Wei, H., Zheng, W., Li, L., Liu, X., Chen, J., Xia, D., Oldknow, C., Ye, W., Chen, F., 2020a. Differential ice volume and orbital modulation of Quaternary moisture patterns between Central and East Asia. Earth Planet. Sci. Lett. 530, 115901.
Li, J., Yu, R., Zhou, T., 2008. Teleconnection between NAO and climate downstream of the Tibetan Plateau. J. Clim. 21, 4680–4690.
Li, L., Sokolik, I.N., 2018. Analysis of dust aerosol retrievals using satellite data in Central Asia. Atmosphere 9, 288.
Li, Y., Song, Y., 2021. Discussion of the paper "Loess genesis and worldwide distribution" by Yanrong Li, Wenhui Shi, Adnan Aydin, et al. Earth-Sci. Rev. 221, 103151.
Li, Y., Song, Y., Fitzsimmons, K.E., Chang, H., Orozbaev, R., Li, X., 2018a. Eolian dust dispersal patterns since the last glacial period in eastern Central Asia: insights from a loess-paleosol sequence in the Ili Basin. Clim. Past. 14, 271–286.
Li, Y., Song, Y., Fitzsimmons, K.E., Chen, X., Wang, Q., Sun, H., Zhang, Z., 2018b. New evidence for the provenance and formation of loess deposits in the Ili River Basin. Arid Central Asia. Aeolian Res. 35, 1–8.
Li, Y., Song, Y., Kaskaoutis, D.G., Chen, X., Mamadjanov, Y., Tan, L., 2019a. Atmospheric dust dynamics in southern Central Asia: implications for buildup of Tajikistan loess sediments. Atmos. Res. 229, 74–85.
Li, Y., Song, Y., Lai, Z., Han, L., An, Z., 2016a. Rapid and cyclic dust accumulation during MIS 2 in Central Asia inferred from loess OSL dating and grain-size analysis. Sci. Rep. 6, 32365.
Li, Y., Song, Y., Orozbaev, R., Dong, J., Li, X., Zhou, J., 2020b. Moisture evolution in Central Asia since 26 ka: insights from a Kyrgyz loess section, Western Tian Shan. Quat. Sci. Rev. 249, 106604.
Li, Y., Song, Y., Qiang, M., Miao, Y., Zeng, M., 2019b. Atmospheric dust variations in the Ili Basin, Northwest China, during the last glacial period as revealed by a high mountain loess-paleosol sequence. J. Geophys. Res.: Atmosph. 124 (15), 8449–8466.
Li, Y., Song, Y.G., Chen, X.L., Li, J.C., Mamadjanov, Y., Aminov, J., 2016b. Geochemical composition of Tajikistan loess and its provenance implications. Palaeogeogr. Palaeoclimatol. Palaeoecol. 446, 186–194.
Li, Y., Song, Y., Fitzsimmons, K.E., Chen, X., Prud'homme, C., Zong, X., 2020c. Origin of loess deposits in the North Tian Shan piedmont, Central Asia. Palaeogeogr. Palaeoclimatol. Palaeoecol. 559, 109972.
Li, Y., Song, Y.G., Kaskaoutis, D.G., Zan, J.B., Orozbaev, R., Tan, L.C., Chen, X.L., 2021. Aeolian dust dynamics in the Fergana Valley, Central Asia, since similar to 30 ka inferred from loess deposits. Geosci. Front. 12, 101180. https://doi.org/10.1016/j.gsf.2021.101180.
Li, Y., Song, Y., Yan, L., Chen, T., An, Z., Li, C.-S., 2015. Timing and Spatial Distribution of Loess in Xinjiang, NW China. Plos One 10 (5), e0125492.
Li, Y., Song, Y., Yin, Q., Han, L.i., Wang, Y., 2019c. Orbital and millennial northern mid-latitude westerlies over the last glacial period. Clim. Dyn. 53 (5–6), 3315–3324.
Lioubimtseva, E., Cole, R., Adams, J.M., Kapustin, G., 2005. Impacts of climate and land-cover changes in arid lands of Central Asia. J. Arid Environ. 62 (2), 285–308.
Lisiecki, L.E., Raymo, M.E., 2005. A Pliocene-Pleistocene stack of 57 globally distributed benthic delta O-18 records. Paleoceanography 20, PA1003. https://doi.org/10.1029/2004PA001071.

Liu, J., Ding, J., Rexiding, M., Li, X., Zhang, J., Ran, S.i., Bao, Q., Ge, X., 2021. Characteristics of dust aerosols and identification of dust sources in Xinjiang. China. Atmos. Environ. 262, 118651.
Liu, J., Ding, J., Li, L., Li, X., Zhang, Z., Ran, S.i., Ge, X., Zhang, J., Wang, J., 2020. Characteristics of aerosol optical depth over land types in central Asia. Sci. Total Environ. 727, 138676.
Lu, H., Jia, J., Yin, Q.Z., Xia, D.S., Gao, F.Y., Liu, H., Fan, Y.J., Li, Z.J., Wang, X., Berger, A., Oimuhammadzoda, I., Gadoev, M., 2020. Atmospheric dynamics patterns in southern central Asia Since 800 ka revealed by loess-paleosol sequences in Tajikistan. Geophys. Res. Lett., 47 https://doi.org/10.1029/2020GL088320.
Luetscher, M., Boch, R., Sodemann, H., Spotl, C., Cheng, H., Edwards, R.L., Frisia, S., Hof, F., Muller, W., 2015. North Atlantic storm track changes during the Last Glacial Maximum recorded by Alpine speleothems. Nat. Commun. 6, 6344.
Lydolph, P.E., 1977. Climates of the Soviet Union, World Survey of Climatology. Elsevier, Amsterdam.
Machalett, B., Oches, E.A., Frechen, M., Zöller, L., Hambach, U., Mavlyanova, N.G., Marković, S.B., Endlicher, W., 2008. Aeolian dust dynamics in central Asia during the Pleistocene: driven by the long-term migration, seasonality, and permanency of the Asiatic polar front. Geochem. Geophys. Geosyst. 9 (8).
Maher, B.A., Prospero, J.M., Mackie, D., Gaiero, D., Hesse, P.P., Balkanski, Y., 2010. Global connections between aeolian dust, climate and ocean biogeochemistry at the present day and at the last glacial maximum. Earth-Sci. Rev. 99 (1-2), 61–97.
Marx, S.K., Kamber, B.S., McGowan, H.A., Petherick, L.M., McTainsh, G.H., Stromsoe, N., Hooper, J.N., May, J.-H., 2018. Palaeo-dust records: a window to understanding past environments. Global Planet. Change 165, 13–43.
Meyer-Christoffer, A., Becker, A., Finger, P., Schneider, U., Ziese, M., 2018. GPCC climatology version 2018 at 0.25°: monthly land-surface precipitation climatology for every month and the total year from rain-gauges built on GTS-based and historical data. In: Global Precipitation Climatology Centre (GPCC, h.g.d.d.a.D.W. (Ed.), 2018 ed, Offenbach, Germany.
Nobakht, M., Shahgedanova, M., White, K., Altausen, D., Abdullaev, S., Hofer, J., 2019. New inventory of dust sources in Central Asia derived from the daily MODIS imagery. E3S Web Conf. 99, 01001.
Nobakht, M., Shahgedanova, M., White, K., 2021. New inventory of dust emission sources in central Asia and northwestern China derived from MODIS imagery using dust enhancement technique. J. Geophys. Res.: Atmosph. 126 (4).
Ogi, M., Tachibana, Y., Yamazaki, K., 2003. Impact of the wintertime North Atlantic Oscillation (NAO) on the summertime atmospheric circulation. Geophys. Res. Lett. 30, 1704. https://doi.org/10.1029/2003GL017280.
Opp, C., Groll, M., Aslanov, I., Lotz, T., Vereshagina, N., 2017. Aeolian dust deposition in the southern Aral Sea region (Uzbekistan): ground-based monitoring results from the LUCA project. Quat. Int. 429, 86–99.
Orlovsky, L., Orlovsky, N., 2002. White sand storms in Central Asia. Global Alarm: Dust and Sand Storms from the World's Dry lands. UNCCD, Bangkok, 169–201.
Orlovsky, L., Orlovsky, N., Durdyev, A., 2005. Dust storms in Turkmenistan. J. Arid Environ. 60 (1), 83–97.
Orlovsky, N.S., Indoitu, R., 2013. Severe dust storms in Central Asia. Arid Ecosyst. 3 (4), 227–234.
Panagiotopoulos, F., Shahgedanova, M., Hannachi, A., Stephenson, D.B., 2005. Observed trends and teleconnections of the Siberian high: a recently declining center of action. J. Clim. 18, 1411–1422.
Papadimas, C., Hatzianastassiou, N., Mihalopoulos, N., Querol, X., Vardavas, I., 2008. Spatial and temporal variability in aerosol properties over the Mediterranean basin based on 6-year (2000–2006) MODIS data. J. Geophys. Res.: Atmosph. 113. https://doi.org/10.1029/2007JD009189.
Pausata, F.S.R., Li, C., Wettstein, J.J., Kageyama, M., Nisancioglu, K.H., 2011. The key role of topography in altering North Atlantic atmospheric circulation during the last glacial period. Clim. Past. 7, 1089–1101.
Perşoiu, A., Ionita, M., Weiss, H., 2019. Atmospheric blocking induced by the strengthened Siberian High led to drying in west Asia during the 4.2 ka BP event–a hypothesis. Clim. Past. 15, 781–793.
Pi, H., Sharratt, B., Lei, J., 2017. Atmospheric dust events in central Asia: relationship to wind, soil type, and land use. J. Geophys. Res.: Atmosph. 122, 6652–6671.
Prospero, J.M., Ginoux, P., Torres, O., Nicholson, S.E., Gill, T.E., 2002. Environmental characterization of global sources of atmospheric soil dust identified with the Nimbus 7 Total Ozone Mapping Spectrometer (TOMS) absorbing aerosol product. Rev. Geophys. 40 (1), 2-1–2-31.
Rachkovskaya, E.I., 2003. Botanical-geographic types of deserts, In: Rachkovskaya, E. I., Volkov, E.A., Khramtsov, V.N. (Eds.), Botanical Geography of Kazakhstan and Middle Asia (Desert Region), pp. 26–28.
Raible, C.C., Yoshimori, M., Stocker, T.F., Casty, C., 2007. Extreme midlatitude cyclones and their implications for precipitation and wind speed extremes in simulations of the Maunder Minimum versus present day conditions. Clim. Dyn. 28 (4), 409–423.
Rashki, A., Kaskaoutis, D., Sepehr, A., 2018. Statistical evaluation of the dust events at selected stations in Southwest Asia: From the Caspian Sea to the Arabian Sea. Catena 165, 590–603.
Riviere, G., Laine, A., Lapeyre, G., Salas-Melia, D., Kageyama, M., 2010. Links between rossby wave breaking and the north atlantic oscillation-arctic oscillation in present-day and last glacial maximum climate simulations. J. Clim. 23, 2987–3008.
Rivière, G., Orlanski, I., 2007. Characteristics of the Atlantic storm-track eddy activity and its relation with the North Atlantic Oscillation. J. Atmos. Sci. 64, 241–266.
Roe, G., 2009. On the interpretation of Chinese loess as a paleoclimate indicator. Quat. Res. 71 (2), 150–161.
Rugenstein, J.K.C., Chamberlain, C.P., 2018. The evolution of hydroclimate in Asia over the Cenozoic: a stable-isotope perspective. Earth-Sci. Rev. 185, 1129–1156.
Rupakheti, D., Rupakheti, M., Abdullaev, S.F., Yin, X., Kang, S., 2020. Columnar aerosol properties and radiative effects over Dushanbe, Tajikistan in Central Asia. Environ. Pollut. 265, 114872.
Sahsamanoglou, H.S., Makrogiannis, T.J., Kallimopoulos, P.P., 1991. Some aspects of the basic characteristics of the siberian anticyclone. Int. J. Climatol. 11 (8), 827–839.
Schettler, G., Shabunin, A., Kemnitz, H., Knoeller, K., Imashev, S., Rybin, A., Wetzel, H. U., 2014. Seasonal and diurnal variations in dust characteristics on the northern slopes of the Tien Shan - Grain-size, mineralogy, chemical signatures and isotope composition of attached nitrate. J. Asian Earth Sci. 88, 257–276.
Serno, S., Winckler, G., Anderson, R.F., Jaccard, S.L., Kienast, S.S., Haug, G.H., 2017. Change in dust seasonality as the primary driver for orbital-scale dust storm variability in East Asia. Geophys. Res. Lett. 44 (8), 3796–3805.
Sha, Y., Shi, Z., Liu, X., An, Z., Li, X., Chang, H., 2018. Role of the Tian Shan mountains and pamir plateau in increasing spatiotemporal differentiation of precipitation over interior Asia. J. Clim. 31 (19), 8141–8162.
Shen, H., Abuduwaili, J., Samat, A., Ma, L., 2016. A review on the research of modern aeolian dust in Central Asia. Arab. J. Geosci. 9, 1–16.
Shi, L., Zhang, J., Yao, F., Zhang, D.a., Guo, H., 2021. Drivers to dust emissions over dust belt from 1980 to 2018 and their variation in two global warming phases. Sci. Tot. Environ. 767, 144860.
Shi, L., Zhang, J., Yao, F., Zhang, D.a., Guo, H., 2020. Temporal variation of dust emissions in dust sources over Central Asia in recent decades and the climate linkages. Atmos. Environ. 222, 117176.
Shindell, D.T., Schmidt, G.A., Mann, M.E., Rind, D., Waple, A., 2001. Solar forcing of regional climate change during the Maunder Minimum. Science 294 (5549), 2149–2152.
Sima, A., Kageyama, M., Rousseau, D.D., Ramstein, G., Balkanski, Y., Antoine, P., Hatte, C., 2013. Modeling dust emission response to North Atlantic millennial-scale climate variations from the perspective of East European MIS 3 loess deposits. Clim. Past. 9, 1385–1402.
Singhvi, A.K., Bluszcz, A., Bateman, M.D., Rao, M.S., 2001. Luminescence dating of loess–palaeosol sequences and coversands: methodological aspects and palaeoclimatic implications. Earth-Sci. Rev. 54 (1–3), 193–211.
Small, E.E., Giorgi, F., Sloan, L.C., 1999. Regional climate model simulation of precipitation in central Asia: mean and interannual variability. J. Geophys. Res.: Atmosph. 104, 6563–6582.
Smalley, I., Mavlyanova, N., Rakhmatullaev, K.L., Shermatov, M.S., Machalett, B., Dhand, K.H., Jefferson, I., 2006. The formation of loess deposits in the Tashkent region and parts of Central Asia; and problems with irrigation, hydrocollapse and soil erosion. Quat. Int. 152, 59–69.
Song, Y., Li, Y., Cheng, L., Zong, X., Kang, S., Ghafarpour, A., Li, X., Sun, H., Fu, X., Dong, J., Mamadjanov, Y., Orozbaev, R., Shukurov, N., Gholami, H., Shukurov, S., Xie, M., 2021. Spatio-temporal distribution of Quaternary loess across Central Asia. Palaeogeogr. Palaeoclimatol. Palaeoecol. 567, 110279.
Song, Y., Nie, J., Song, C., Zan, J., 2022. Cenozoic climatic and environmental changes in Central Asia. Palaeogeography, Palaeoclimatology, Palaeoecology 597, 111012. https://doi.org/10.1016/j.palaeo.2022.111012.
Song, Y., Zeng, M., Chen, X., Li, Y., Chang, H., An, Z., Guo, X., 2018. Abrupt climatic events recorded by the Ili loess during the last glaciation in Central Asia: evidence from grain-size and minerals. J. Asian Earth Sci. 155, 58–67.
Song, Y.G., Chen, X.L., Qian, L.B., Li, C.X., Li, Y., Li, X.X., Chang, H., An, Z.S., 2014. Distribution and composition of loess sediments in the Ili Basin, Central Asia. Quat. Int. 334, 61–73.
Sun, Y.B., An, Z.S., 2005. Late Pliocene-Pleistocene changes in mass accumulation rates of eolian deposits on the central Chinese Loess Plateau. J. Geophys. Res.: Atmosph., 110
Sun, Y., Wang, X., Liu, Q., Clemens, S.C., 2010. Impacts of post-depositional processes on rapid monsoon signals recorded by the last glacial loess deposits of northern China. Earth Planet. Sci. Lett. 289 (1–2), 171–179.
Sung, M.K., Kwon, W.T., Baek, H.J., Boo, K.O., Lim, G.H., Kug, J.S., 2006. A possible impact of the North Atlantic Oscillation on the East Asian summer monsoon precipitation. Geophys. Res Lett., 33
Thompson, D.W.J., Wallace, J.M., 1998. The Arctic Oscillation signature in the wintertime geopotential height and temperature fields. Geophys. Res. Lett. 25 (9), 1297–1300.
Tian, S., Sun, J., Zhang, Z., Abdulov, S., Cao, M., Gadoev, M., Oimahmadov, I., 2021. Loess deposits in the Tajik Basin, Central Asia: chronology, provenance and palaeoclimatic implications since the Last Glacial. Boreas 50 (1), 147–166.
Újvári, G., Stevens, T., Molnár, M., Demény, A., Lambert, F., Varga, G., Jull, A.T., Páll-Gergely, B., Buylaert, J.-P., Kovács, J., 2017. Coupled European and Greenland last glacial dust activity driven by North Atlantic climate. Proc. Nat. Acad. Sci. 114 (50), E10632–E10638 https://doi.org/10.1073/pnas.1712651114.
Vandenberghe, J., French, H.M., Gorbunov, A., Marchenko, S., Velichko, A.A., Jin, H.J., Cui, Z.J., Zhang, T.J., Wan, X.D., 2014. The Last Permafrost Maximum (LPM) map of the Northern Hemisphere: permafrost extent and mean annual air temperatures, 25–17ka BP. Boreas 43, 652–666.
Vandenberghe, J., Renssen, H., van Huissteden, K.o., Nugteren, G., Konert, M., Lu, H., Dodonov, A., Buylaert, J.-P., 2006. Penetration of Atlantic westerly winds into Central and East Asia. Quat. Sci. Rev. 25 (17–18), 2380–2389.

Wang, F., Li, Z., Wang, X., Li, B., Chen, F., 2018a. Variation and interplay of the Siberian High and westerlies in central-east Asia during the past 1200 kyr. Aeolian Res. 33, 62–81.
Wang, H., Zhou, W., Shu, P., Hong, B., An, Z., 2021. Two-stage evolution of glacial-period Asian monsoon circulation by shifts of westerly jet streams and changes of North American ice sheets. Earth-Sci. Rev. 215, 103558.
Wang, L., Jia, J., Li, G., Li, Z., Wang, X., Chen, F., 2018b. Fine-grained quartz OSL dating chronology of loess sequence from southern Tajikistan: implications for climate change in arid central Asia during MIS 2. J. Asian Earth Sci. 155, 116–123.
Wang, S., Zhang, M., Che, Y., Chen, F., Qiang, F., 2016. Contribution of recycled moisture to precipitation in oases of arid central Asia: a stable isotope approach. Water Resour. Res. 52 (4), 3246–3257.
Wu, B.Y., Wang, J., 2002. Possible impacts of winter Arctic Oscillation on Siberian high, the East Asian winter monsoon and sea-ice extent. Adv. Atmos. Sci. 19 (2), 297–320.
Xi, X., Sokolik, I.N., 2015a. Dust interannual variability and trend in Central Asia from 2000 to 2014 and their climatic linkages. J. Geophys. Res.: Atmosph. 120, 12,175–112,197.
Xi, X., Sokolik, I.N., 2015b. Seasonal dynamics of threshold friction velocity and dust emission in Central Asia. J. Geophys. Res.: Atmosph. 120 (4), 1536–1564.
Yang, S., Ding, F., Ding, Z., 2006. Pleistocene chemical weathering history of Asian arid and semi-arid regions recorded in loess deposits of China and Tajikistan. Geochim. Cosmochim. Acta 70 (7), 1695–1709.
Yang, S., Liu, N., Li, D., Cheng, T., Liu, W., Li, S., Chen, H., Liu, L.i., Luo, Y., 2021. Quartz OSL chronology of the loess deposits in the Western Qinling Mountains, China, and their palaeoenvironmental implications since the Last Glacial period. Boreas 50 (1), 294–307.
Yu, L., Lai, Z., 2012. OSL chronology and palaeoclimatic implications of aeolian sediments in the eastern Qaidam Basin of the northeastern Qinghai-Tibetan Plateau. Palaeogeog. Palaeoclimatol. Palaeoecol. 337, 120–129.
Zhang, T., Han, W., Han, Y., Lü, S., Madsen, D., Yu, L., Yang, S., Wang, Y., 2021. What drove late Holocene dust activity in central Asia, natural processes or human activity? Palaeogeogr. Palaeoclimatol. Palaeoecol. 578, 110585.
Zhang, X.-X., Claiborn, C., Lei, J.-Q., Vaughan, J., Wu, S.-X., Li, S.-Y., Liu, L.-Y., Wang, Z.-F., Wang, Y.-D., Huang, S.-Y., Zhou, J., 2020. Aeolian dust in Central Asia: spatial distribution and temporal variability. Atmos. Environ. 238, 117734.
Zhao, L., Jin, H., Li, C., Cui, Z., Chang, X., Marchenko, S.S., Vandenberghe, J., Zhang, T., Luo, D., Guo, D., Liu, G., Yi, C., 2014. The extent of permafrost in China during the local Last Glacial Maximum (LLGM). Boreas 43 (3), 688–698.
Zhou, L.P., Dodonov, A.E., Shackleton, N.J., 1995. Thermoluminescence dating of the Orkutsay loess section in Tashkent region, Uzbekistan, Central Asia. Quat. Sci. Rev. 14 (7–8), 721–730.

Yue Li received his Ph.D. from University of Chinese Academy of Sciences in 2020 and now works at Institute of Earth Environment, Chinese Academy of Sciences (CAS), as Special Research Assistant of CAS. He had been a visiting scholar in Max Planck Institute of Chemistry (Germany, 2017). He did his graduate work (PhD) in sedimentology, element geochemistry and clay mineralogy of Central Asian loess. He incorporated meteorological data and mathematical statistical methods into investigations of Central Asian loess to establish the physical loess-climate (sub)system linkages and quantify source contributions of loess deposits, and explored paleoclimate changes in North Tianshan region and underlying driving mechanisms herein. He has published 31 peer-reviewed papers, and therein, eleven SCI papers and one EI paper papers were published as the first author. His research interests include quantifying the provenance of Central Asian loess, loess-based dust dynamics, and driving mechanism of moisture evolution in the Westerly-dominated Central Asia.

Yougui Song is a professor of Quaternary Geology in Institute of Earth Environment, CAS. He obtained his M. Sc. (1998) in Quaternary geology from Nanjing University, and Ph.D. (2001) in physical geography from Lanzhou University. Subsequently, he carried out late Cenozoic aeolian sediments and geomorphological evolutions in Chinese Loess Plateau at Institute of Earth Environment, CAS as a postdoctoral fellow. He was a visiting scholar at Kyoto University (Japan), Utrecht University (Netherland), University of Rhode Island (USA), and Baylor University (USA). His current research interests are loess, palaeoclimate and environmental changes in Central Asia and Northwest China. He has published about 180 peer-reviewed articles (over 100 in science citation index journals). He is also a guest-editor, academic editor or editorial board number of several international journals such as Palaeogeography, Palaeoclimatology, Palaeoecology, Quaternary International, Plos One.

Dimitris G. Kaskaoutis received his Ph.D. from the University of Ioannina, Greece in 2009. After serving 5 years as professor in Indian Universities, from 2017 onward he is Research Assistant at the National Observatory of Athens. His research interests focus on solar radiation transfer into the atmosphere, aerosol physical, chemical and optical properties, carbonaceous aerosols and climate implications, meteorology, air quality and natural hazards (dust storms, biomass burning). He has published 150 papers in scientific journals with more than 4500 citations by others, 8 Book Chapters and he has served as reviewer in many scientific journals.

Xiaoxiao Zhang completed his Ph.D. at Beijing Normal University in 2010. During 2010–2019, he served as assistant research fellow at Xinjiang Institute of Ecology and Geography, CAS. He had been a visiting scholar at University of Nebraska, USA, from 2011 to 2012, and at Washington State University, USA, from 2018 to 2019. He is currently working on Xinjiang Institute of Ecology and Geography, CAS, as a Research Associate Professor. His research interests include atmospheric environment in arid and semi-arid areas and aeolian dust variability in Central Asia.

Xiuling Chen received her Ph.D. degree in physical geography from Lanzhou University (China, 2005). She did her graduate work (PhD) in elemental geochemistry of aeolian deposits and Quaternary environmental evolution. From 2010, she is an associate professor at the College of Geographical Sciences, Fujian Normal University, and successively served as deputy head of the Department of Resources and Urban Planning and the Department of Geography. Her research areas are environmental evolution and human countermeasures, geochemistry and sediment provenance tracing, heavy metal and rare earth element contamination.

Nosir Shukurov obtained his Ph.D. from Tashkent State University in 2000. Subsequently he did post-doctoral research at Bar-Ilan University (Israel). From 2004, he returned to work at the Institute of Geology and Geophysics of the Uzbekistan Academy of Sciences, and served as the deputy director of the institute. He has been a visiting scholar at University of Bayreuth (Germany); Johannes Gutenberg University of Mainz (Germany); University of Athens (Greece); University of Bern (Switzerland); University of the West Indies (Jamaica); University of Georgia (USA). Currently he is working as a head of the Geochemistry lab. at the Kh.M. Abdullaev's Institute of Geology and Geophysics, University of Geological Sciences, State Committee of the Republic of Uzbekistan for Geology and Mineral Resources. His research interest includes Environmental Sciences, Environmental Geochemistry, environmental pollution assessment, Heavy metals in soils, concentrations, chemical and mineralogical forms, and their bioavailability.

Rustam Orozbaev obtained a PhD degree in Geology at the Shimane University (Japan, 2010). He was awarded Japan Society for the Promotion of Science (JSPS) fellowship and carried out the research at the Kyoto University (Japan, 2012–2014). Currently he works as a senior research scientist at the Institute of Geology, National Academy of Sciences of Kyrgyz Republic. His research areas are geology, metamorphic petrology, geochemistry, tectonics, mining, and environmental geology of the Tien-Shan Mts. in Central Asia.